ANTIOXIDANTS & REDOX SIGNALING
Volume 16, Number 1, 2012

DOI: 10.1089/ars.2011.3933

ORIGINAL RESEARCH COMMUNICATION

Glutaredoxin S12: Unique Properties for Redox Signaling

Mirko Zaffagnini,[1,2] Mariette Bedhomme,[1] Christophe H. Marchand,[1] Jérémy Couturier,[3] Xing-Huang Gao,[1] Nicolas Rouhier,[3] Paolo Trost,[2] and Stéphane D. Lemaire[1]

Abstract

Aims: Cysteines (Cys) made acidic by the protein environment are generally sensitive to pro-oxidant molecules. Glutathionylation is a post-translational modification that can occur by spontaneous reaction of reduced glutathione (GSH) with oxidized Cys as sulfenic acids (-SOH). The reverse reaction (deglutathionylation) is strongly stimulated by glutaredoxins (Grx) and requires a reductant, often GSH. ***Results:*** Here, we show that chloroplast GrxS12 from poplar efficiently reacts with glutathionylated substrates in a GSH-dependent ping pong mechanism. The pK_a of GrxS12 catalytic Cys is very low (3.9) and makes GrxS12 itself sensitive to oxidation by H_2O_2 and to direct glutathionylation by nitrosoglutathione. Glutathionylated-GrxS12 (GrxS12-SSG) is temporarily inactive until it is deglutathionylated by GSH. The equilibrium between GrxS12 and glutathione ($E_{m(GrxS12\text{-}SSG)} = -315$ mV, pH 7.0) is characterized by K_{ox} values of 310 at pH 7.0, as in darkened chloroplasts, and 69 at pH 7.9, as in illuminated chloroplasts. ***Innovation:*** Based on thermodynamic data, GrxS12-SSG is predicted to accumulate *in vivo* under conditions of mild oxidation of the GSH pool that may occur under stress. Moreover, GrxS12-SSG is predicted to be more stable in chloroplasts in the dark than in the light. ***Conclusion:*** These peculiar catalytic and thermodynamic properties could allow GrxS12 to act as a stress-related redox sensor, thus allowing glutathione to play a signaling role through glutathionylation of GrxS12 target proteins. *Antioxid. Redox Signal*. 16, 17–32.

Introduction

In plant cells, glutathione (γ-GluCysGly) is the most abundant nonprotein thiol (15). It is present in many subcellular compartments, including chloroplasts where it can reach the concentration of 1–4.5 m*M*, and serves as a major antioxidant to keep the intracellular environment reduced (44). Moreover, glutathione provides electrons to the ascorbate cycle and to some thiol-peroxidases and is, therefore, important for the detoxification of several compounds including reactive oxygen species (16). In chloroplasts as in other compartments, glutathione is maintained in the reduced state by NADPH-dependent glutathione reductase (GR). Although in most physiological conditions intracellular glutathione is essentially in the reduced form (GSH), it can be converted to the oxidized form (GSSG) under oxidative stress conditions (16, 44).

Recently, glutathione has been found to be involved in a reversible post-translational modification termed glutathionylation, which is mainly promoted by oxidative and nitrosative stresses (22). This modification, consisting in the formation of a mixed disulfide between glutathione and a protein cysteine (Cys) residue, is typically considered a mechanism of protection of specific Cys residues from irreversible oxidation to sulfinic (-SO_2H) or sulfonic (-SO_3H) acids (22). Besides protection, glutathionylation can also constitute a mode of regulation, as it can modulate the activity of target enzymes and thereby play a role in many cellular processes (11). Glutathionylation has been extensively studied in mammalian cells, and emerging evidence suggests that it could constitute an important mechanism of regulation and signaling in plants as well (20, 34, 44, 53). Whether glutathionylation is important for protection or regulation *in vivo*, the modification needs to be removed when the stress conditions or the signaling

Innovation

Glutathionylation is an emerging post-translational modification that could play an important role in cell regulation and signaling. Deglutathionylation reactions are mainly controlled by glutaredoxins (Grx). This study shows that higher plant chloroplastic GrxS12 exhibits peculiar catalytic and thermodynamic properties that could allow this enzyme to act as a stress-related redox sensor allowing glutathione to play a signaling role through glutathionylation of GrxS12 target proteins.

[1]Laboratoire de Biologie Moléculaire et Cellulaire des Eucaryotes, FRE3354 Centre National de la Recherche Scientifique, Institut de Biologie Physico-Chimique, Université Pierre et Marie Curies, Paris, France.
[2]Department of Experimental Evolutionary Biology, University of Bologna, Bologna, Italy.
[3]Unité Mixte de Recherches 1136 Nancy Université—INRA Interaction Arbres—Microorganismes, IFR 110 EFABA, Faculté des Sciences, Vandoeuvre Cedex, France.

event is over. This process, named deglutathionylation, is mainly catalyzed by glutaredoxins (Grx) (23).

Grx are small ubiquitous oxidoreductases belonging to the thioredoxin family and bearing in their active site a characteristic four-amino acids motif with one or two reactive cysteines (CXXC/S). Although thioredoxins mainly serve as protein disulfide reductases, Grxs interact specifically with the GSH moiety of proteins containing glutathione-mixed disulfides (23, 54). In mammalian Grxs, the deglutathionylation reaction was shown to start with the nucleophilic attack of the glutathionyl sulfur of the substrate by the N-terminal Cys of Grx active site (18). The reaction releases the target protein in its reduced form but generates a glutathionylated Grx intermediate that is reduced back by GSH with concomitant formation of GSSG (Fig. 1) (14, 46). This latter reaction may constitute the rate-limiting step of the overall process (46).

In higher plants, three classes of Grxs have been initially defined based on their active site sequences (30, 42, 43), and the classification has been recently refined after identifying a fourth class (8). Class I includes proteins with CXX(C/S) active site other than CGFS and are also named CPYC-type because of the most common active site motif. Class II contains exclusively Grxs with a CGFS motif (CGFS-type), class III, which is specific to land plants, corresponds to Grxs with a peculiar CCX(C/S) active site (CC-type), and class IV regroups peculiar proteins composed of a Grx domain with CXXC/S active site and two additional domains of unknown functions in the C-terminal part. Here, we report the biochemical characterization of a chloroplastic Grx isoform from poplar (GrxS12) which belongs to class I and possesses an unusual ^{28}WCSYS^{32} active site sequence and a second C-terminal Cys (Cys87) that are both conserved in orthologs from other plant species. Class I contains 6 members in poplar and Arabidopsis (41, 44), GrxS12 being the only one lacking the second Cys in the active site sequence motif. The *x*-ray crystal structure of glutathionylated GrxS12 from poplar was recently solved (9) and found to contain a single GSH molecule covalently bound to active site Cys29. Interestingly, C-terminal Cys87 was found to be located at proximity of the active site, though not interacting with bound GSH. Since Cys87 formed no disulfide with either Cys29 or GSH, and the GrxS12-C87S (C87S) mutated variant displayed a similar deglutathionylating activity as the wild-type protein, a monothiol mechanism based on active site Cys29 was proposed for GrxS12 (Fig. 1) (9). By contrast, some Grxs display a dithiol mechanism, as they use a second Cys in the deglutathionylation reaction. This was recently demonstrated for *Chlamydomonas reinhardtii* Grx3 (CGFS-type), in which removal of the glutathionyl moiety from the N-terminal Cys of Grx active site is performed by a second Cys of the same monomer, equivalent to Cys87 of GrxS12 (54). The resulting intramolecular disulfide was found to possess a low redox potential (−323 mV at pH 7.9) and to be insensitive to glutathione, whereas it could be reduced by ferredoxin:thioredoxin reductase (FTR) under photosynthetic conditions.

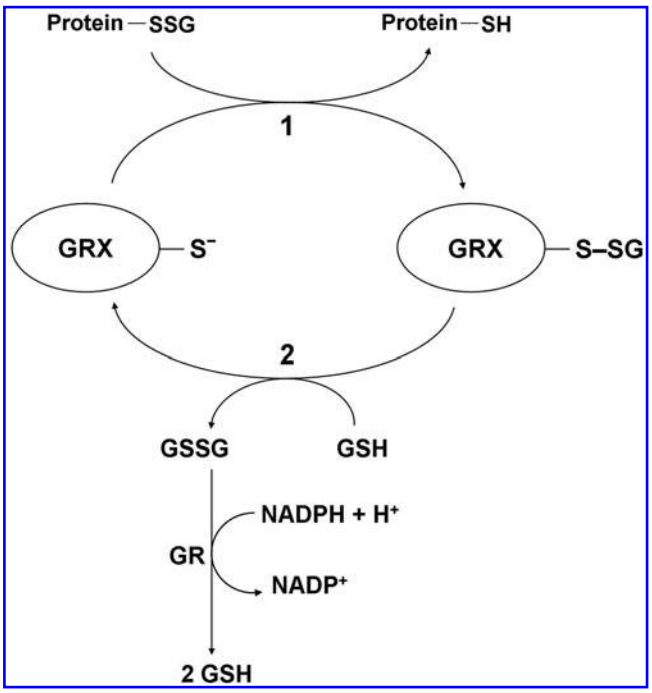

FIG. 1. Schematic representation of the deglutathionylation activity of Grxs. The reaction mechanism here depicted is a monothiol mechanism, as a single cysteine (Cys) of the glutaredoxin (Grx) is involved in catalysis. The overall reaction catalyzed by Grx consists of two steps: nucleophilic attack of the glutathionyl sulphur of the glutathionylated substrate (protein-SSG) by Grx thiolate (step 1) and nucleophilic attack of the glutathionyl sulphur of the glutathionylated Grx (Grx-SSG) by reduced glutathione (also in thiolate form, step 2). Regeneration of glutathione (GSH) by glutathione reductase (GR) allows determination of Grx activity as NADPH oxidation rate. For *in vitro* assays of Grx activity, the glutathionylated protein (protein-SSG) can be substituted by glutathionylated β-mercaptoethanol (β-ME-SSG) in the classical hydroxyethyldisulfide (HED) assay.

The present article shows that protein deglutathionylation catalyzed by poplar GrxS12 follows a ping-pong mechanism. The reaction, based on Cys29, is highly sensitive to [GSH]/[GSSG] ratios and proceeds at maximal rates only when glutathione is extensively reduced. Typical of Grxs, catalytic Cys29 was found to be extremely acidic ($pK_a = 3.9$) and, thus, sensitive to alkylation and to oxidation by H_2O_2, besides undergoing glutathionylation in the presence of glutathionylated substrates or nitrosoglutathione (GSNO). The GrxS12-catalyzed deglutathionylation reaction is strongly stimulated by alkaline pH, thus possibly reflecting the important role of deprotonated glutathione (GS^-) in the attack of glutathionylated GrxS12 (step 2, Fig. 1). The standard redox potential of the mixed disulfide of glutathionylated GrxS12, to our knowledge the first measured among Grxs, is −350 mV at pH 7.9, a typical pH value for photosynthesizing chloroplasts (47). Owing to its monothiol mechanism, to the low pK_a of catalytic Cys29, and to the low redox potential of the mixed disulfide, glutathionylated GrxS12 may accumulate *in vivo* under stress conditions, when the GR potential is much less reducing than −350 mV. These unique biochemical properties could allow GrxS12 to act as a stress-related redox sensor, thus allowing glutathione to play a signaling role through glutathionylation of GrxS12 target proteins.

Results

Poplar GrxS12 follows a ping-pong reaction mechanism

Artificial substrates such as glutathionylated β-mercaptoethanol (β-ME-SSG) produced by the spontaneous reaction

Table 1. Apparent Kinetic Parameters of the Deglutathionylating Activity of GrxS12 and C87S Mutant with Different Substrates

	HED[a]		*BSA-SSG*[b]		*GSH*[c]	
Protein	$K_{m(HED)}$ μM	k_{cat} s^{-1}	$K_{m(BSA\text{-}SSG)}$ μM	k_{cat} s^{-1}	$K_{m(GSH)}$ μM	k_{cat} s^{-1}
GrxS12	310 ± 40	23.1 ± 0.9	26.6 ± 1.8	31.3 ± 2.5	$(4.0 \pm 0.5) \times 10^{3}$[d]	92.8 ± 5.3[d]
C87S	300 ± 30	26.5 ± 1.1	28.4 ± 2.4	33.9 ± 1.2	$(3.1 \pm 0.1) \times 10^{3}$	102.8 ± 6.4

Deglutathionylation activities of GrxS12 and C87S were determined with 30 n*M* glutaredoxin as described under "Materials and Methods" section. Apparent K_m and k_{cat} values for each substrate were calculated by nonlinear regression using the Michaelis-Menten equation. Data are represented as means ± SD ($n = 3$).

[a]HED concentration was varied (from 0.1 to 1.5 m*M*), and the GSH concentration was maintained at 1 m*M*.

[b]BSA-SSG concentration was varied (from 2.5 to 50 μM), and the GSH concentration was maintained at 1 m*M*.

[c]GSH concentration was varied (from 0.5 to 3.5 m*M*), and the HED concentration was maintained at 0.7 m*M*.

[d]Values taken from Ref. (8).

BSA-SSG, glutathionylated bovine serum albumin; GSH, glutathione; HED, hydroxyethyldisulfide; SD, standard deviation.

of GSH with hydroxyethyldisulfide (HED) are routinely used in Grx activity assays (9, 21, 54). Based on this standard assay, purified GrxS12 displayed a specific activity of 70 μmol min^{-1} mg^{-1} and site-specific mutant C87S performed similarly (66 μmol min^{-1} mg^{-1}), whereas the specific activity of mutant C29S was very low (3.2 μmol min^{-1} mg^{-1}), thus confirming the essential role of Cys29 and the negligible role of Cys87 in GrxS12 catalysis. In the presence of 1 m*M* GSH, GrxS12 displayed an apparent K_m for HED of 0.3 m*M* and a turnover number of 23 s^{-1} (Table 1). Under similar conditions (1 m*M* GSH), the K_m of GrxS12 for glutathionylated bovine serum albumin (BSA-SSG) was ten-fold lower (K_m 27 μM), whereas the apparent turnover number was only slightly higher (31 s^{-1}) (Table 1). Apparent kinetic parameters of site-specific mutant C87S were very similar to those measured for the wild-type protein (Table 1).

A two-substrate kinetic analysis of GrxS12 was performed with BSA-SSG and GSH. Plots of initial velocities *versus* substrate concentrations were hyperbolic, although not saturated at the highest concentrations of either fixed substrate (Fig. 2A, B). Double reciprocal plots generated parallel line patterns, characteristic of a ping-pong mechanism (Fig. 2C, D). This implies that after the interaction of GrxS12 with BSA-SSG, reduced BSA is released before GSH can reduce the mixed disulfide of GrxS12-SSG (see Fig. 1). When apparent k_{cat} values obtained from nonlinear regression of original data were plotted as a function of substrate concentration, responses were approximately linear rather than hyperbolic (Fig. 2A, B). This effect prevented any reliable determination of true kinetic parameters k_{cat} and K_m *via* nonlinear regression. Indeed, secondary plots $1/k_{cat}$ *versus* 1/[BSA-SSG] or 1/[GSH] projected to the origin, indicating that true K_m and k_{cat} values are too high to be experimentally determined (insets in Fig. 2A, B). On the other hand, since k_{cat}/K_m ratios in ping-pong mechanisms are not influenced by the concentration of the second substrate (a property that is visually represented by the parallelism of double reciprocal plots), the catalytic efficiency parameter k_{cat}/K_m could be precisely derived from kinetic data of Figure 2. These true kinetic parameters were $(2.5 \pm 0.1) \times 10^{4}$ M^{-1} s^{-1} for GSH and $(8.0 \pm 0.6) \times 10^{5}$ M^{-1} s^{-1} for BSA-SSG, thereby implying that the true K_m for BSA-SSG was 30-times lower than for GSH. In spite of some variability in experimental conditions, GrxS12 catalytic efficiency (with both HED and BSA-SSG) appeared roughly comparable with previously characterized Grx from human (18, 27), yeast (12), and *C. reinhardtii* (21, 54).

Glutathionylated isocitrate lyase is efficiently reactivated by GrxS12

Assays of Grx activity with HED or BSA-SSG as substrates are based on the capacity of Grx to transfer a GSH moiety from a glutathionylated substrate to free GSH, thereby generating GSSG that is reduced by GR (see Fig. 1). Alternatively, GRX deglutathionylating activity can be directly assayed by measuring the reactivation of an enzyme whose activity is affected by glutathionylation. Isocitrate lyase (ICL) from *C. reinhardtii* provides such an opportunity, as this enzyme, which undergoes glutathionylation *in vivo* (35), was recently shown to be reversibly inhibited by glutathionylation of its active site Cys (3). Glutathionylated ICL (ICL-SSG; ≈ 100% inactivated) was, thus, used as a model substrate; and GrxS12 was tested for its ability to restore ICL activity in the presence of a suitable electron donor (Fig. 3). Again, mutant C87S behaved identical to wild-type GrxS12 in ICL-SSG reactivation, whereas the activity of mutant C29S was 5% of the wild type and not further investigated (not shown).

In control experiments, 20 m*M* dithiothreitol (DTT) alone allowed full chemical reactivation of ICL-SSG (10 μM) in 5 min, but lower concentrations of DTT (*e.g.*, 0.5 m*M*) were much less efficient (Fig. 3A). In the absence of external reductants, reduced GrxS12 (5 μM) caused very rapid but partial reactivation of ICL-SSG (Fig. 3A). In the presence of both DTT (0.5 m*M*) and GrxS12 (5 μM), reactivation of ICL-SSG (10 μM) proceeded at a slightly faster rate than with GrxS12 alone and continued until ICL was fully activated (Fig. 3A).

Similar experiments were performed with GSH as a physiological reductant instead of DTT. In the absence of GrxS12, very slow reactivation was promoted by 2 m*M* GSH alone, which contained about 1% oxidized glutathione as a contaminant (*i.e.*, 20 μM GSSG). Under these conditions, addition of 5 μM GrxS12 increased the initial velocity of ICL-SSG reactivation (Fig. 3B), but still reactivation kinetics with GSH was much slower than with DTT (Fig. 3A). Reactivation of ICL-SSG by GrxS12 and GSH (contaminated by 1% GSSG) depended on GrxS12 concentration with an $S_{0.5}$ of 4.5 μM (Fig. 3C).

To check the effect of GSSG contamination on GrxS12 activity, a GSH-regenerating system (GRS) based on GR and NADPH was applied to guarantee full reduction of GSH. The GRS had no detectable effects on the nonenzymatic reactivation of ICL-SSG by GSH (Fig. 3B), but strongly stimulated ICL-SSG reactivation by 5 μM GrxS12 (Fig. 3B). Moreover, the $S_{0.5}$ for

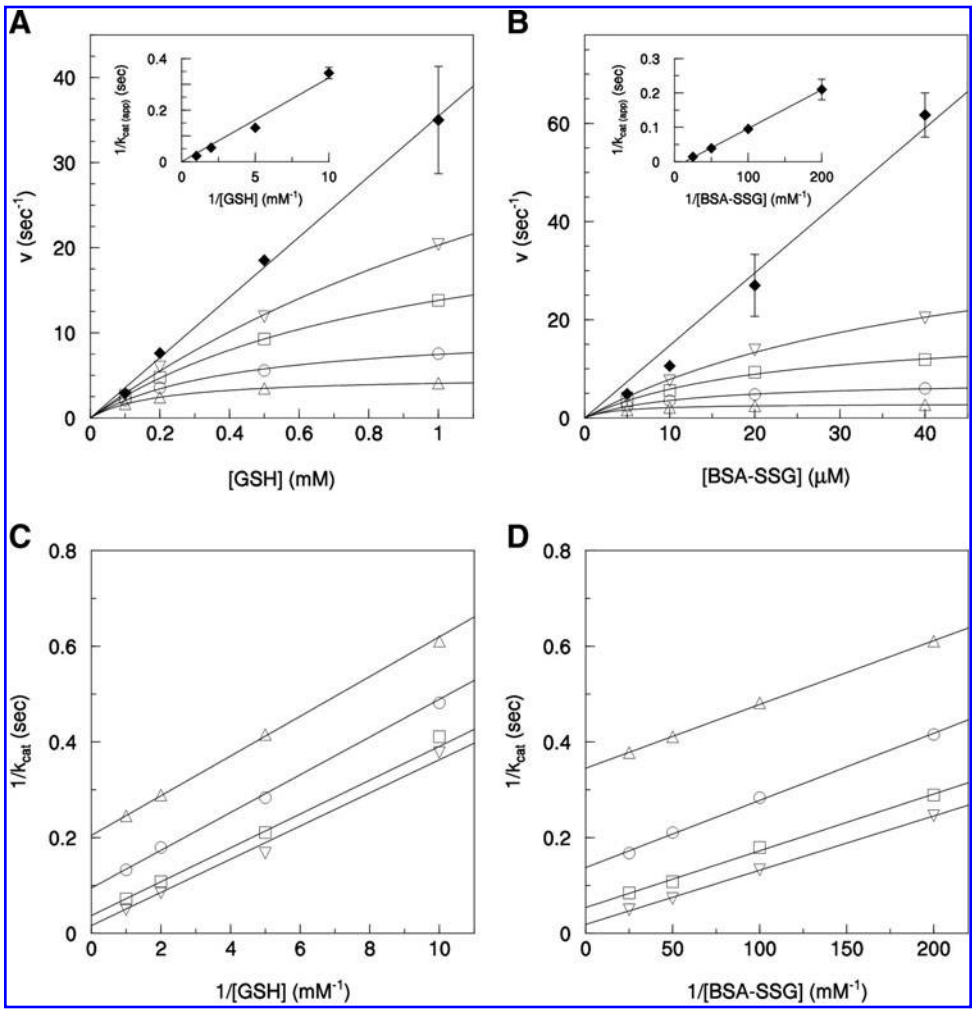

FIG. 2. Two-substrate kinetic analysis of GrxS12-dependent deglutathionylation reactions reveals a ping-pong kinetic mechanism. (A) Deglutathionylation of glutathionylated bovine serum albumin (BSA-SSG) by GrxS12 (30 n*M*) in the presence of fixed BSA-SSG concentrations with varied GSH concentrations (*open symbols*). Data points represent the average of three experiments, and standard deviations (SDs) are omitted for clarity. From top to bottom: 40, 20, 10, 5 μM BSA-SSG. *Closed diamonds* represent apparent k_{cat} values extrapolated from *panel* **(B)** (mean ± SD of individual experiments). *Inset* show secondary plots of the reciprocal apparent k_{cat} *versus* the reciprocal of GSH concentration. **(B)** Deglutathionylation of BSA-SSG by GrxS12 in the presence of fixed concentrations of GSH with varied BSA-SSG concentrations (*open symbols*). Data points represent the average of three experiments, and SDs are omitted for clarity. From top to bottom: 1, 0.5, 0.2, 0.1 m*M* GSH. *Closed diamonds* represent apparent k_{cat} values extrapolated from *panel* **(A)** (mean ± SD of individual experiments). *Inset* show secondary plots of the reciprocal apparent k_{cat} *versus* the reciprocal of BSA-SSG concentration. **(C)** Double reciprocal plots of data shown in *panel* **(A)**. Interpolating lines are defined by Lineweaver-Burk linear equations including the apparent kinetic parameters obtained by nonlinear regression of the original data in *panel* **(A)**. **(D)** Double reciprocal plots of data shown in *panel* **(B)**. Interpolating lines are defined by Lineweaver-Burk linear equations including the apparent kinetic parameters obtained by nonlinear regression of the original data in *panel* **(B)**.

GrxS12 determined in the presence of 2 m*M* fully reduced GSH (*i.e.,* GRS) was as low as 0.1 μM (Fig. 3D); and time-course reactivation of ICL-SSG (10 μM) by 0.1 μM GrxS12 and fully reduced GSH followed a similar kinetics as with 5 μM GrxS12 and partially reduced GSH (Fig. 3B).

To better understand the role of GSSG, different [GSH]/[GSSG] ratios were then tested. In Figure 3D, [GSH]/[GSSG] ratios were corrected for the unavoidable contamination of GSSG in fresh GSH solutions. Such a contamination fixed a practical limit to the highest [GSH]/[GSSG] ratio that could be tested. As shown in Figure 3D, after 15 min incubation, any [GSH]/[GSSG] ratio below 100 had the effect of decreasing the deglutathionylating activity of GrxS12; and no significant activity was detected at [GSH]/[GSSG] ratios below 5. On the other hand, complete and fast reactivation of ICL-SSG required [GSH]/[GSSG] ratios higher than 100 that could only be obtained by the GRS (Fig. 3B). The effect of GSSG was mainly on GrxS12, as reduced ICL was only marginally inhibited by any of the [GSH]/[GSSG] ratios tested in Figure 3D (not shown).

Catalytic Cys29 of GrxS12 is very acidic (pK_a 3.9)

Catalytic efficiency of Grxs, similar to other thiol-dependent oxidoreductases, may largely depend on the reactivity of the catalytic Cys, which, in turn, depends on its acidity. The pK_a of the thiol group of catalytic Cys29 was previously estimated as ~2.8 by following the pH-dependent interaction of the C87S mutant with the thiol-cleavable fluorophore (2-pyridyl)di-thiobimane (PDT-bimane) (9). Provided that the monothiol catalytic mechanism of GrxS12 is based on Cys29, we have re-determined the pK_a of this Cys by following the activity of wild-type GrxS12 after treatment with the thiolate-alkylating agent iodoacetamide (IAM) (18, 36).

By plotting the residual activity *versus* pH (corrected for the pH-dependency of GrxS12 activity in the absence of IAM), a complete sigmoid titration curve was obtained, which gave an accurate pK_a value of 3.93 ± 0.09 for the inactivation reaction (Fig. 4). Analysis of C87S mutant (pK_a 3.82 ± 0.11) fully confirmed this value (Fig. 4). Though confirming that Cys29 is extremely acidic, the difference with the previous estimation

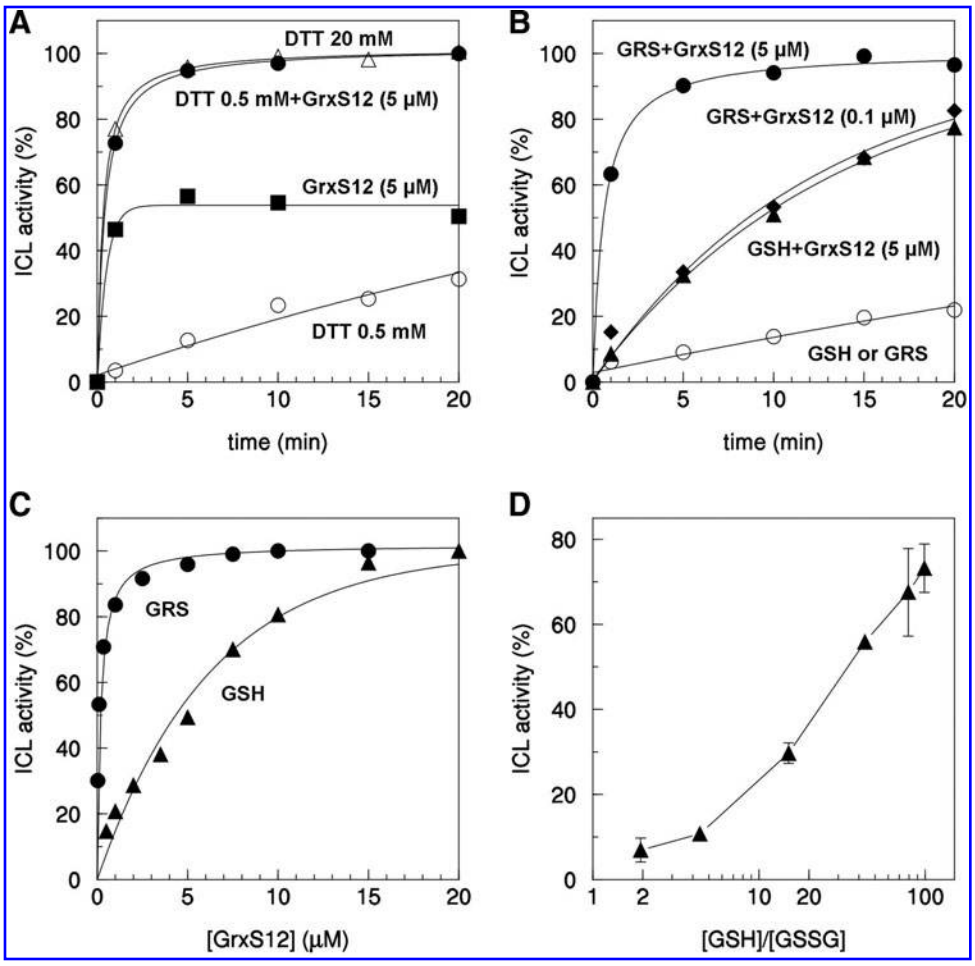

FIG. 3. Reactivation of glutathionylated isocitrate lyase (ICL-SSG) by GrxS12. (A) ICL-SSG was incubated with dithiothreitol (DTT) alone (0.5 m*M*, *open circles*; or 20 m*M*, *open triangles*) or with 5 μM reduced GrxS12 alone (*black squares*) or with 0.5 m*M* DTT plus 5 μM GrxS12 (*black circles*). During incubation, aliquots were withdrawn from the medium and immediately assayed for ICL activity. **(B)** Reactivation in the presence of GSH. ICL-SSG was incubated with 2 m*M* GSH alone or with a GSH-regenerating system (GRS: 2 m*M* GSH, 0.2 m*M* NADPH, 6 μg/ml GR), which provided full and constant reduction of GSH (*white circles*). Alternatively, ICL-SSG was incubated with 5 μM GrxS12 plus 2 m*M* GSH alone (*black triangles*) or 5 μM GrxS12 plus GRS (*black circles*). Reactivation of ICL-SSG was also carried out in the presence of 0.1 μM GrxS12 and GRS (*black diamonds*). **(C)** Reactivation of ICL-SSG as a function of GrxS12 concentration and reducing system (either 2 m*M* GSH, *black triangles*; or GRS, *black circles*). ICL activity was measured immediately after a constant incubation of 10 min for each sample. **(D)** Reactivation of ICL-SSG after 15 min incubation with 5 μM GrxS12 in the presence of different [GSH]/[GSSG] ratios. In each *panel*, ICL activities are expressed as a percentage of the maximal ICL activity measured after incubation with 20 m*M* DTT for 10 min. Data points represent the average of at least three experiments. Except for *panel* **(D)**, SDs were omitted for clarity.

of Cys29 pK_a (9) is most probably related to the use of different measurement methods. In particular, the reduction of PDT-bimane disulfide by protein thiolates is slow under extremely acidic conditions and requires very long incubations [up to 2 h, see Ref. (9)] that may affect protein stability. Under these conditions, the use of IAM may be advantageous, as alkylation of protein thiolates by IAM is not pH-sensitive and it is fast enough to require a few minutes of incubation (3 min, Fig. 4). We, thus, suggest that pK_a determination of very acidic Cys performed by IAM may be more reliable compared with the method based on the cleavable fluorophore PDT-bimane.

GrxS12-catalyzed deglutathionylation is strongly stimulated by alkaline pH

The rate of GrxS12-catalyzed deglutathionylation of β-ME-SSG (HED assay) was found to be strongly pH-dependent. The activity was negligible at pH 6.5 and reached its maximum above pH 9 (Fig. 5). The inflection point of the interpolating curve was around 8.2. Such a response was only observed in the presence of a large excess of GR (90 μg/ml) in the coupled assay. In the presence of lower amounts of GR (6 μg/ml), as in the standard HED assay, the pH-rate profile was bell shaped (Fig. 5). Since the pH optimum of yeast GR is around 6.5 (7), the apparent inhibition of GrxS12 activity at alkaline pH was thought to derive from the inhibition of GR, which limited, in turn, the overall reaction. In fact, by increasing the concentration of GR, such inhibition could be overcome, and the pH-rate dependence became sigmoidal (Fig. 5).

Since thiol dissociation is a general prerequisite for the nucleophilic attack of disulfides (26), the inflection point of the sigmoidal pH-rate response should reflect the pK_a of the thiol involved in the limiting step of the overall reaction. The three thiols involved have very distinct pK_a values: GrxS12-thiol is very acidic (pK_a 3.9; Fig. 4), whereas the pK_a of β-ME-SH is very alkaline (9.8) (46) and exceeds by more than one unit that of GSH (8.7) (46). Since the pK_a of GSH (8.7) is the closest to 8.2, we tentatively conclude that the nucleophilic attack made by GS^- on GrxS12-SSG (step 2 in Fig. 1) should limit the overall reaction catalyzed by GrxS12 under these conditions (Fig. 5).

GrxS12 is sensitive to alkylation and oxidation, but not nitrosylation

The reactivity of GrxS12 *versus* IAM was further characterized at the pH value normally used for plant Grx activity assays (pH 7.9), conditions leading to full dissociation of Cys29 (pK_a 3.9). Incubation of GrxS12 with variable amounts

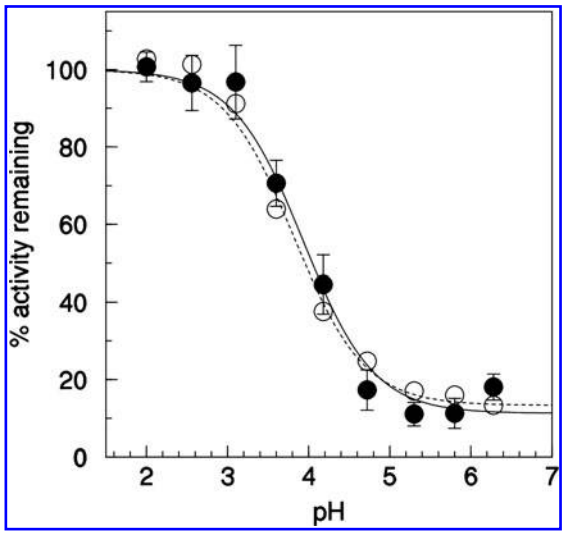

FIG. 4. Determination of the pK_a of the active site Cys of GrxS12. Reduced GrxS12 (3 μM, *black circles*) and C87S mutant (3 μM, *white circles*) were incubated with iodoacetamide (IAM) (0.3 mM) at different pH values for 3 min at room temperature and then assayed using the standard HED assay after 100-fold dilution. After incubation, the percentages of remaining activity at each pH were determined by comparing the activity of the enzyme incubated with and without IAM. *Symbols* represent the average of at least three experiments ± SDs. For the sake of clarity, SDs for C87S mutant data were omitted. The pK_a values were obtained by nonlinear regression using an adaptation of the Henderson-Hasselbalch equation (16). Interpolation curves for GrxS12 and C87S mutant are represented as full and dashed sigmoids, respectively.

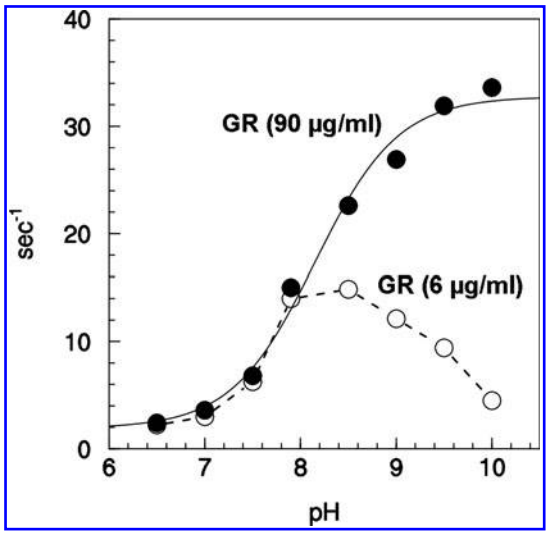

FIG. 5. pH-rate profile of GrxS12 activity. The activity of GrxS12 was assayed with HED. The concentration of GR in the assay was either the standard concentration for the HED assay (6 μg/ml, *open circles*), or 15-fold increased (90 μg/ml, *black circles*). Buffers were potassium phosphate (pH 6.5–7.5), Tris-HCl (pH 7.5–9), and glycine (pH 9–10). GrxS12-dependent deglutathionylating activity is represented as a percentage of maximal activity. Interpolation of experimental data with GR in excess (*black circles*) was made by nonlinear regression with the Henderson-Hasselbalch equation.

of IAM caused inactivation of GrxS12 after a pseudo-first-order kinetics (Fig. 6A), which enabled apparent first-order constants (k_{app}) to be determined. Kitz-Wilson analysis of the data was used to generate the limiting constants for inactivation (k_{inact}) and K_I (dissociation constant) (Fig. 6C and Table 2) (29). The same conditions were used to compare the effect of alkylation by IAM with the effect of oxidation by H_2O_2, a reaction that is also known to be favored by the thiolate state of Cys (38). GrxS12 was inactivated by H_2O_2 in a time- and concentration-dependent manner (Fig. 6B). Kitz-Wilson analysis (Fig. 6C) revealed that, based on second-order rate constants (k_{inact}/K_I; Table 2), H_2O_2 was 12-fold less efficient than IAM as an inhibitor of GrxS12.

H_2O_2-dependent inhibition of GrxS12 is likely related to the oxidation of Cys residues into sulfenic acids (primary oxidation) that can be further irreversibly oxidized to sulfinic and sulfonic acids. In GrxS12, glutathionylation of Cys29 was detected by matrix-assisted laser desorption/ionization-time of flight (MALDI-TOF) mass spectrometry after spontaneous reaction with H_2O_2 and GSH. The resulting mixed disulfide on GrxS12 was very stable and could only be reduced back by fully reduced GSH or DTT (9). Here, we show that after GrxS12 inactivation by H_2O_2 (0.1 mM, 15 min) to 60% of its original activity, reactivation by a GRS was complete (Fig. 7). This result indicated that under these conditions, H_2O_2 caused only primary oxidation to sulfenic acid such that GSH could quantitatively regenerate active glutathionylated GrxS12. Consistently, no inhibition was observed when GrxS12 was treated with H_2O_2 (0.1 mM) in the presence of GSH (0.5 mM) (Fig. 7). By contrast, treatments with higher concentrations of H_2O_2 (1 mM) for the same time led to 80% inhibition of GrxS12 and only partial reactivation by the GRS (Fig. 7), suggesting that, under these harsher conditions, part of the catalytic Cys was irreversibly oxidized most likely to the sulfinate and/or sulfonate forms.

To investigate whether GrxS12 can be a target of nitrosylation, we treated the protein with GSNO, a typical NO-donor. The reaction of GrxS12 with GSNO under aerobic conditions had no effect on its activity (Fig. 7). Further, GSNO treatment did not induce any absorption band at 335 nm, characteristic for S-nitrosothiol groups (data not shown). Altogether, these results suggest that neither Cys29 nor Cys87 may be nitrosylated under these conditions. However, GSNO can also induce the formation of glutathione-mixed disulfides. MALDI-TOF mass spectrometry analysis revealed a mass increase of ~305 Da in the totality of GrxS12 treated with GSNO, consistent with the formation of one glutathione adduct. The 305 Da mass increase was reversed by treatment with DTT (Fig. 8).

The midpoint redox potential of glutathionylated GrxS12 is −349 mV at the pH of 7.9 (as in illuminated chloroplasts) and −315 mV at pH 7.0 (as in darkened chloroplasts)

Due to the large shift of 305 Da in molecular mass, MALDI-TOF mass spectrometry allows to unambiguously quantify the ratio between reduced and glutathionylated GrxS12 under different conditions. We used this method to characterize the equilibrium between GrxS12 and GSH redox buffer. Experiments were performed at pH 7.9, a value that might occur in chloroplasts under photosynthetic conditions (47). Ratios between reduced and glutathionylated GrxS12 were determined

after equilibration with different GSH/GSSG ratios (Fig. 9A) according to the following reaction:

$$\text{GrxS12-SH} + \text{GSSG} \leftrightarrow \text{GrxS12-SSG} + \text{GSH}$$

The equilibrium constant of GrxS12 oxidation by GSSG (K_{ox}) could be derived from the equilibrium concentration of the different species (Fig. 9B):

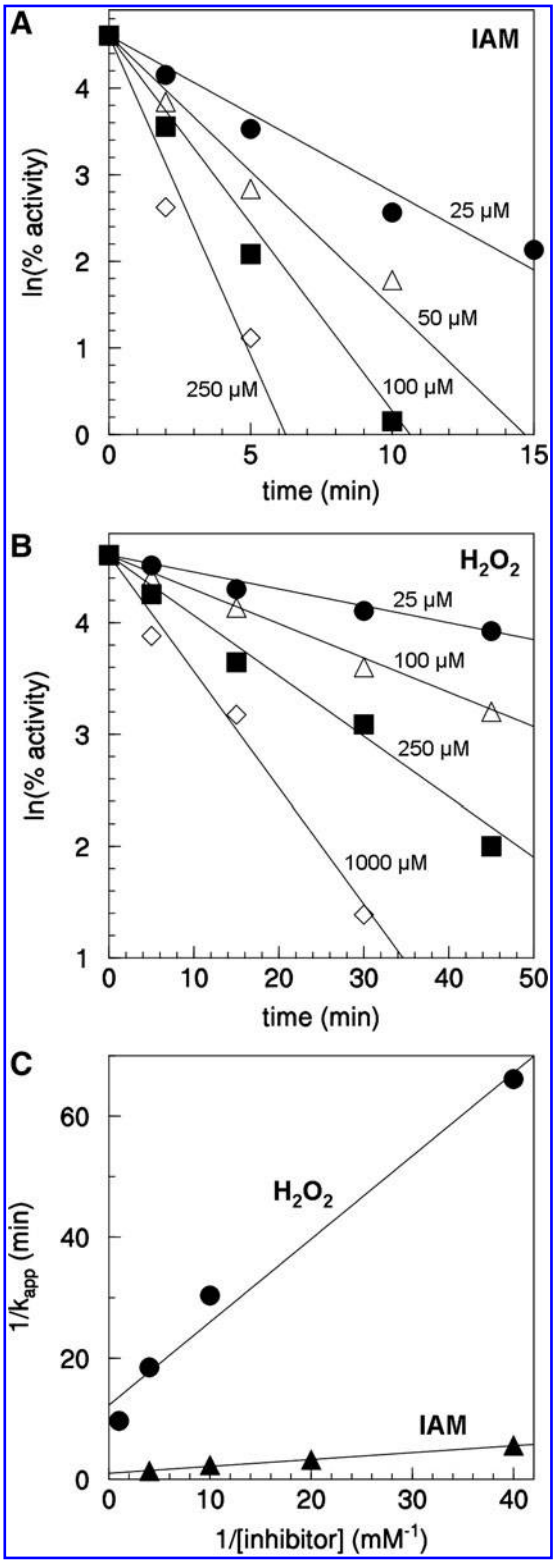

Table 2. Kinetic Parameters for Inhibition of GrxS12 by Iodoacetamide and H_2O_2

Compound	K_I μM	k_{inact} min^{-1}	k_{inact}/K_I $M^{-1}\,min^{-1}$
IAM	114 ± 13	1.00 ± 0.06	8.77×10^3
H_2O_2	112 ± 20	0.082 ± 0.006	7.32×10^2

The kinetic parameters of GrxS12 inhibition by IAM and H_2O_2 were determined by incubating the protein with variable amounts of inactivator. At different times, aliquots were withdrawn to assay glutaredoxin activity using HED assay with 30 n*M* GrxS12. K_I and k_{inact} were determined according to (26). Data are represented as means ± SD ($n = 3$).

IAM, iodoacetamide.

$$K_{ox} = [\text{GrxS12-SSG}]/[\text{GrxS12-SH}] \times [\text{GSH}]/[\text{GSSG}]$$

Based on three independent experiments, the average K_{ox} resulted to be 69 ± 12 standard deviation (SD). The E_m of GrxS12 mixed disulfide could then be derived from the K_{ox} by means of the Nernst equation:

$$E_{m(\text{GrxS12 - SSG})} = E_{m(\text{GSSG})} - RT/nF \times \ln K_{ox}$$

Considering an $E_{m(GSSG)}$ of −294 mV at pH 7.9 (1) and setting the value of n at 2 (as expected for a disulfide/dithiol two-electron transfer process), the K_{ox} value could then be translated into a midpoint redox potential of GrxS12 mixed disulfide ($E_{m[GrxS12\text{-}SSG]}$) of −349 ± 2 mV.

Then, intrinsic tryptophan fluorescence was used as an alternative method to determine reduced and glutathionylated GrxS12. Fluorescence emission of GrxS12 after excitation at 290 nm was previously reported to be quenched by glutathionylation (9). The minimum distance between the aromatic ring of the only tryptophan of GrxS12 (Trp28) and the mixed disulfide is 3.74 Å, as calculated from the crystal structure of glutathionylated GrxS12 (9) (Fig. 10A). Short-distance interactions between tryptophan aromatic rings and sulfur atoms of disulfides result in intrinsic fluorescence quenching; reduced sulphydryl groups being much less effective (10). Therefore, we compared the fluorescence signal of glutathionylated and reduced GrxS12 after tryptophan-specific excitation at 295 nm (Fig. 10B) and took advantage of this important quenching effect to investigate the redox

FIG. 6. Kinetics of inactivation of GrxS12. The reaction was initiated by the addition of varying concentrations of inactivator (IAM or H_2O_2) to solutions containing reduced GrxS12 in Tris-HCl, pH 7.9. At the indicated time, aliquots were withdrawn from the incubation mixtures and assayed for GrxS12 activity as described in "Material and Methods" Section. **(A)** Time- and concentration-dependent inactivation of GrxS12 by IAM. From top to bottom: 25, 50, 100, 250 μM IAM. **(B)** Time- and concentration-dependent inactivation of GrxS12 by H_2O_2. From top to bottom: 25, 100, 250, 1000 μM H_2O_2. **(C)** Double-reciprocal plots of k_{app} *versus* IAM (*black triangles*) and H_2O_2 (*black circles*) concentrations obtained according to Kitz and Wilson (26) to yield K_I and k_{inact}. Each data point represents the mean of three independently obtained data sets. The straight lines represent the best-fit linear regression through the raw data.

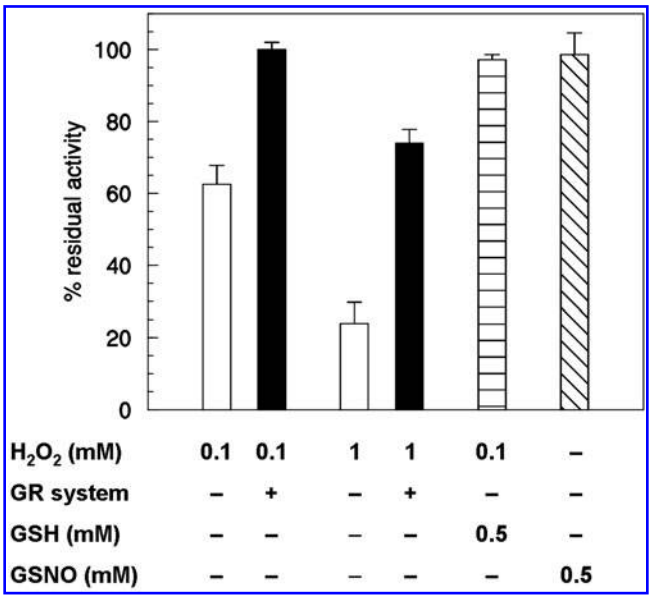

FIG. 7. Effects of oxidants on the activity of GrxS12. After 15 min treatment of GrxS12 with 0.1 or 1 m*M* H_2O_2 (*white bars*) or 0.1 m*M* H_2O_2 in the presence of 0.5 m*M* GSH (*horizontal dashed bar*) or 0.5 m*M* nitrosoglutathione (GSNO) (*diagonal dashed bar*), the residual activity was measured using the standard HED assay. The reversibility of H_2O_2-dependent effects was investigated after incubation of the oxidized protein in the presence of GR system (1 m*M* GSH, 0.2 m*M* NADPH and 6 μg/ml GR) supplemented with 100 U/ml bovine catalase (*dark bars*). Data represent the average of at least three experiments ± SDs.

properties of GrxS12. To this aim, reduced GrxS12 was equilibrated with a fixed GSH/GSSG ratio of 200 at pH 7.9; and a K_{ox} value of 63 ± 9 was derived from three independent determinations of glutathionylated/reduced GrxS12 under these conditions. This value fully confirms the K_{ox} of 69 ± 12 obtained by MALDI-TOF mass spectrometry at the same pH.

Moreover, since the physiological pH at which GrxS12 could react with the GSH system *in vivo* is expected to be variable, it was interesting to investigate the effect of pH on the K_{ox} measured with GSH. To this aim, pH was varied between 5 and 9 and reduced GrxS12 was equilibrated with a fixed GSH/GSSG ratio of 200. The equilibrium ratio between reduced and glutathionylated GrxS12 was determined by the tryptophan fluorescence method (Fig. 10C). K_{ox} values were found to be strongly pH-dependent, varying from a value of 35 at pH 9 to 1250 at pH 5. Maximal slope of the interpolating curve was observed around neutral pH values, with the K_{ox} increasing approximately 10-fold for a pH decrease of 1 unit. At pH 7, the K_{ox} was 310 and could be translated into a standard redox potential of −315 mV.

Discussion

GrxS12 is a chloroplast Grx conserved in land plants with a typical Grx 3D structure based on the thioredoxin fold (9). Chloroplasts of higher plants, such as poplar and Arabidopsis, appear to contain at least four Grx isoforms named C5 and S12 (CPYC-type), and S14 and S16 (CGFS-type) (41). Although characterization of all these Grx isoforms is far from complete, it is known that GrxS12 can regenerate B-type methionine sulfoxide reductase (MSRB1) and A_4-glyceraldehyde-3-phosphate dehydrogenase by deglutathionylation (9, 49); whereas GrxS14 and GrxS16 can function as scaffold proteins for synthesis, transfer, and delivery of iron-sulfur clusters (2). Whether other Grxs besides GrxS12 are active deglutathionylating agents in chloroplasts of higher plants is possible but not yet proved.

Although GrxS12 belongs to CPYC-type Grx, as the classical dithiol human GRX1 and GRX2 (19), in this plant Grx, the typical C-terminal Cys of the CPYC active site motif is replaced by a serine (CSYS). The capacity of GrxS12 to catalyze deglutathionylation is based on the reactivity of Cys29, which becomes glutathionylated after the interaction between GrxS12 and glutathionylated substrates (9). Although GrxS12 contains a conserved Cys (Cys87) outside the ^{28}WCSYS^{32} sequence motif but located in the proximity of Cys29 in the 3D structure, this residue is not involved in the catalytic cycle (9). Therefore, the only possible reaction mechanism of GrxS12, based on Cys29, is a monothiol mechanism.

The monothiol mechanism of GrxS12 contrasts with the dithiol mechanism used by diverse CGFS Grxs, including *C. reinhardtii* Grx3, the ortholog of GrxS14 from higher plants (44, 48, 54). In this alternative mechanism, the glutathionylated Cys

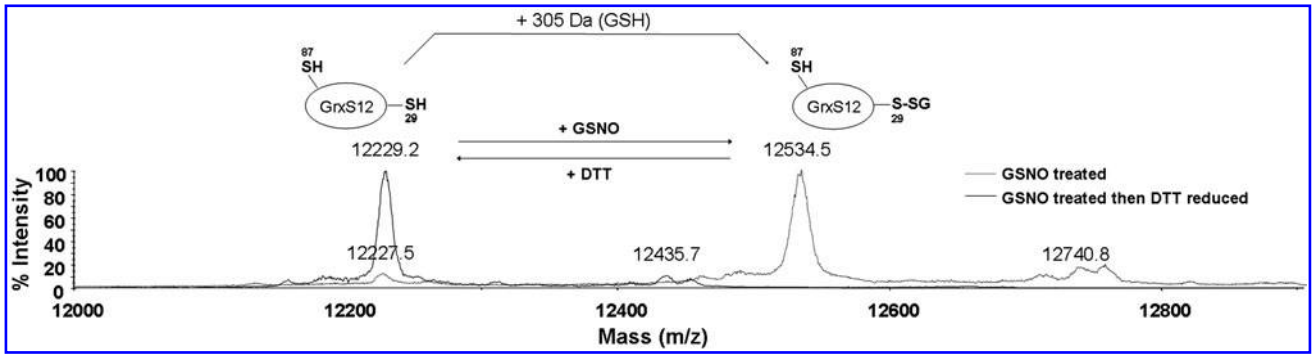

FIG. 8. Matrix-assisted laser desorption/ionization-time of flight (MALDI-TOF) mass spectrometry analysis of GSNO-treated GrxS12. MALDI-TOF spectra of whole protein was determined for reduced GrxS12 before (*full line*) or after (*dotted line*) treatment with 0.5 m*M* GSNO for 1 h at room temperature and desalted using NAP-5 column equilibrated with phosphate-buffered saline, pH 7.4, 1 m*M* EDTA. The 305 Da shift after GSNO treatment could be totally reversed by a treatment with 20 m*M* DTT. The peaks at mass/charge ratio of 12435.7 and 12740.8 correspond to the matrix adducts for the reduced and GSNO-treated GrxS12, respectively.

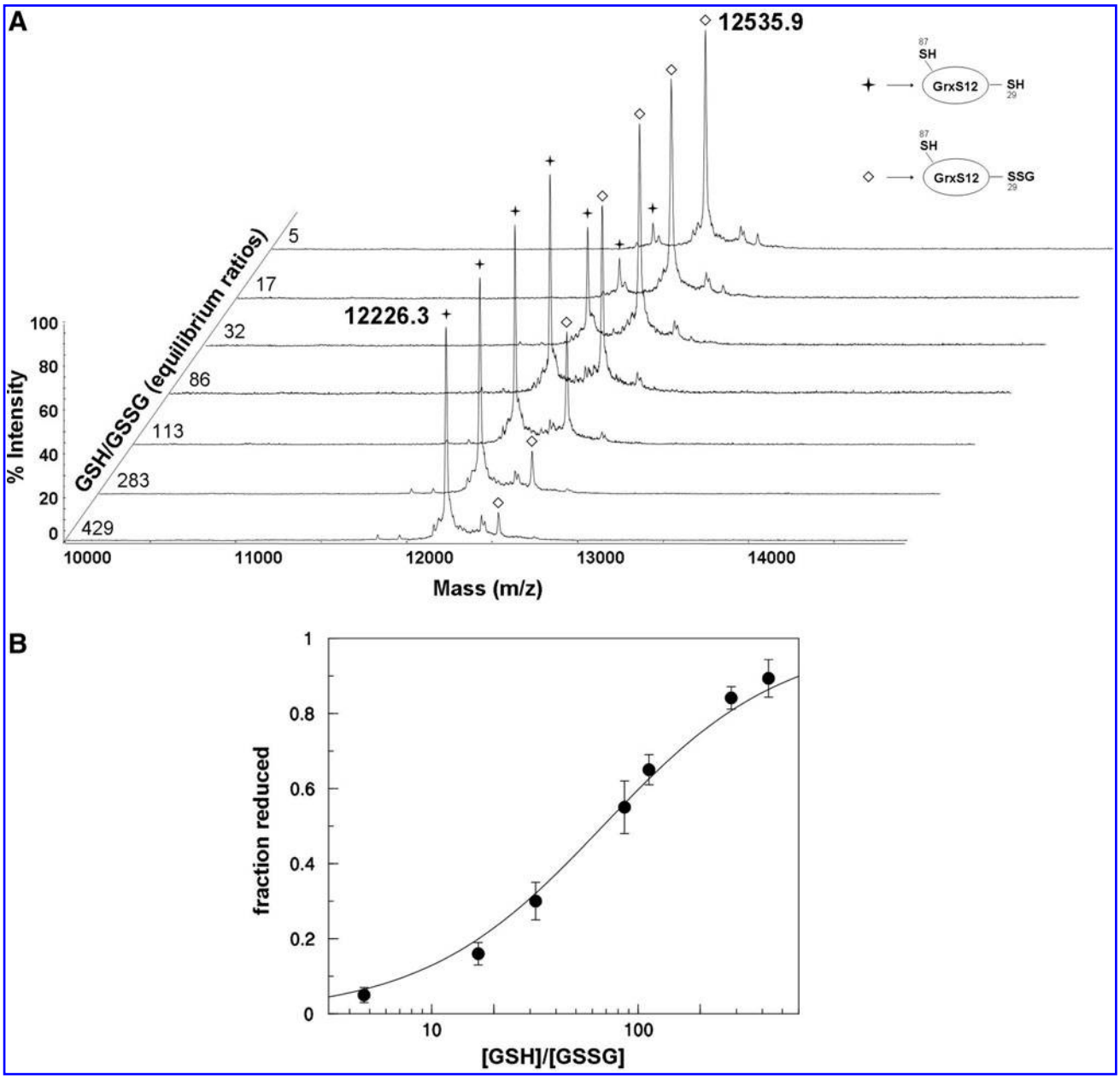

FIG. 9. Redox titration of GrxS12 mixed disulfide with GR buffer. (A) Reduced GrxS12 (50 μM) was equilibrated with different [GSH]/[GSSG] ratios in 30 m*M* Tris-HCl (pH 7.9) for 10 min before the reaction was quenched by 1.3% trifluoroacetic acid. GrxS12-SH/GrxS12-SSG ratios at equilibrium were determined by digital integration of MALDI-TOF mass spectrometry peaks indicated in the figure by *stars* (GrxS12-SH) and *diamonds* (GrxS12-SSG). Spectra are displayed as a function of GSH/GSSG ratios at equilibrium (see Materials and Methods section). A correction was introduced in the calculations to account for the estimated breakage of 5% mixed disulfides by laser shooting. **(B)** The fraction of reduced GrxS12 that was measured by mass spectrometry after equilibration with different glutathione buffers was plotted against the [GSH]/[GSSG] ratio at equilibrium. K_{ox} was obtained from nonlinear least-squares regression. Experimental data are displayed as means ± SD obtained from three separate experiments.

of the Grx is attacked by a second Cys, rather than GSH, with formation of an internal disulfide bridge. In the case of Grx3, the catalytic cycle is closed by the reduction of this disulfide by FTR in a reaction linked to photosynthetic electron transport (54). It is possible that FTR-dependent CGFS-type Grxs and GSH-dependent CPYC-type Grxs co-exist in chloroplasts of higher plants and perform similar reactions, but since they are based on different reducing systems, this might be useful to perform deglutathionylation in both light and dark conditions.

Kinetic properties of GrxS12

The mechanism of deglutathionylation performed by GrxS12 on a glutathionylated protein as BSA is here shown to be ping pong. This mechanism implies that the interaction

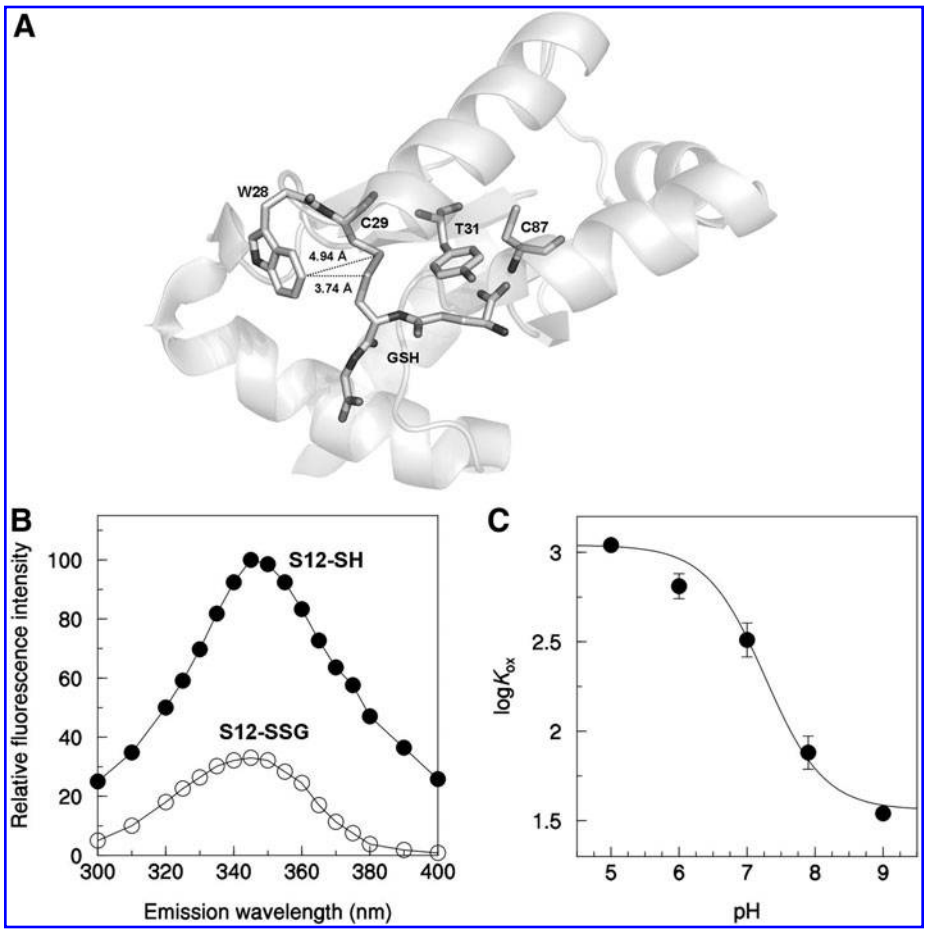

FIG. 10. pH-dependence of GrxS12 K_{ox} with GR buffer. (A) Detail of the crystallographic structure of glutathionylated GrxS12 (8) showing the shortest distances between the aromatic ring of Trp28 and the sulfur atoms of the mixed disulfide. The figure was made with PyMol based on file pdb 3FZ9. **(B)** Emission spectra of reduced (*black circles*) and glutathionylated (*white circles*) GrxS12 (excitation at 295 nm) were recorded with 0.4 μM protein at 25°C in 30 m*M* Tris-HCl, pH 7.9, 1 m*M* EDTA. Buffer blank was run and subtracted from both spectra. The fluorescence maximum of reduced GrxS12 was arbitrarily set to 100 fluorescence units. **(C)** Reduced GrxS12 was equilibrated with an initial [GSH]/[GSSG] ratio of 200:1 (2 m*M* total GSH concentration) at different pH in the following buffers: sodium citrate (pH 5.0), MES (pH 6.0), HEPES (pH 7.0), Tris-HCl (pH 7.9), glycine (pH 9.0). Equilibrium ratios between reduced and glutathionylated GrxS12 were determined by the tryptophan intrinsic fluorescence method. K_{ox} were calculated from equilibrium ratios GSH/GSSG and GrxS12-SSG/GrxS12-SH as described in the text. Data are means ± SD of triplicate determinations.

between reduced GrxS12 and BSA-SSG is followed by the separation between reduced BSA and glutathionylated GrxS12. In the second part of the reaction cycle, GrxS12-SSG reacts with GSH and releases a GSSG molecule while recovering its original reduced state. In all these reactions, thiolates (GrxS12-S^-, GS^-) rather than thiols make the nucleophilic attack on mixed disulfides. Consistently, the reaction catalyzed by GrxS12 was strongly pH dependent and apparently influenced by the limited acidity of GSH (pK_a 8.7) (46). As a consequence, the overall reaction catalyzed by GrxS12 could be limited, at physiological pH values, by the GSH attack on GrxS12-SSG (step 2 of Fig. 1). A similar ping-pong reaction mechanism limited by the GSH attack was demonstrated for both human Grx1 and Grx2 (19). The reaction mechanism of GrxS12 is analogous to human Grxs also for the true kinetic parameters k_{cat} and K_m (*vs.* both BSA-SSG and GSH) being too high to be experimentally determined. However, k_{cat}/K_m ratios of GrxS12 could be determined and found to be in the order of $10^6\ M^{-1}\ s^{-1}$ *versus* BSA-SSG and $10^4\ M^{-1}\ s^{-1}$ *versus* GSH. Similarly, k_{cat}/K_m ratios of human Grx (Grx1, Grx2), though determined under slightly different conditions, were in the range of $10^5\ M^{-1}\ s^{-1}$ *versus* BSA-SSG and 10^4–$10^5\ M^{-1}\ s^{-1}$ *versus* GSH (18, 27). The kinetic features of GrxS12 are consistent with both binary complexes (GrxS12/BSA-SSG and GrxS12-SSG/GSH) being very short living or even nonexistent. Lack of accumulation of binary complexes would explain why GrxS12 could not be experimentally saturated by either substrate. Although the reason for GrxS12-binary complexes being undetectable cannot be derived from present data, it can be safely concluded that GrxS12 practically oscillates between a free reduced form and a free glutathionylated form, with no intermediate complexes, during its catalytic cycle. The fact that free glutathionylated GrxS12 is relatively stable is consistent with its successful crystallization (9).

Thermodynamic properties of GrxS12 and possible physiological roles in vivo

The midpoint redox potential of the glutathionylated GrxS12 mixed disulfide was determined as −349 mV at pH 7.9, a value representative of stromal (chloroplast) pH under photosynthetic conditions (47). This value was obtained by equilibration of GrxS12 with GSH/GSSG as redox buffer and determination of glutathionylated and reduced GrxS12 by MALDI-TOF mass spectrometry (Fig. 9), and confirmed by intrinsic tryptophan fluorescence (Fig. 10).

At pH 7.0, a pH value that represents the chloroplast stroma in the dark, the E_m of GrxS12 mixed disulfide was −315 mV (Fig. 10). The difference of 35 mV between E_m at pH 7.0 and 7.9 is in good agreement with the theory if we consider that at both pH values, catalytic Cys29 of reduced GrxS12 would be deprotonated (pK_a 3.9, Fig. 4), whereas GSH would be mostly protonated (pK_a 8.7) (46). Reduction of GrxS12-SSG mixed

disulfide would, thus, involve two electrons but only one proton, at least at physiological pH:

$$\text{GrxS12-SSG} + 2e^- + 1\ H^+ \rightarrow \text{GrxS12-S}^- + \text{GSH}$$

implying that the standard redox potential of GrxS12 should decrease by ~30 mV for one pH unit increase, very similar to our determinations. To our knowledge, this is the first redox characterization of a mixed disulfide of a wild-type Grx of any source. A variant of yeast Grx1 (CPYC active site), in which the C-terminal Cys of the active site was exchanged to Ser to avoid formation of an internal disulfide and to stabilize the glutathionylated form, was recently reported to have an E_m of −295 mV at pH 7 for the mixed disulfide (25). Other redox analyses, performed on dithiol Grxs, generally showed less negative redox potentials usually comprised between −170 and −232 mV at pH 7 (44). On the contrary, the plastidial *Chlamydomonas* Grx3 displays a midpoint redox potential of −323 mV at pH 7.9 (54), but this disulfide is physiologically reduced by FTR (−374 mV at pH 7.9) (24), a stronger reductant than GSH.

At neutral pH, the standard redox potential of glutathione (−240 mV) (1) is much less reducing than that of GrxS12 (−315 mV). However, the glutathione pool is largely reduced *in vivo*, and its actual redox potential might be much lower. In transgenic *Arabidopsis* plants expressing roGFP2 in the cytosol, the GSH/GSSG ratio *in vivo* was estimated to be 10^5 and the redox potential around −320 mV (28, 32), although it is currently unknown whether roGFP2 fluorescence *in vivo* does only reflect the GSH redox state, or may be influenced by other factors (17). Much lower GSH/GSSG ratios of 10–20 were derived from direct determinations of GSH and GSSG in whole plant tissues (17), but these exceedingly low ratios are hardly representative of the cytosol or chloroplasts, as most of GSSG is likely sequestered in compartments with low reducing capacity (*e.g.*, vacuoles; (39). Whatever the actual GSH/GSSG ratio is under optimal conditions, plenty of evidence demonstrate that the glutathione system *in vivo* is subject to oxidation on stress or when components of the antioxidant system of plants are genetically repressed [(28, 33); for a review see Ref. (17)]. In spite of this, the amplitude of the GSH/GSSG variation in given compartments such as chloroplasts is still uncertain.

Based on our K_{ox} determinations for the reaction of GrxS12 with GSSG (309 at pH 7.0 and 69 at pH 7.9), it can be easily calculated that GrxS12 would be almost completely reduced at any physiological pH if it was in equilibrium with a GSH/GSSG ratio of 10^5. Under these conditions, GrxS12 could efficiently work as a deglutathionylating agent, if necessary. On the other hand, a very limited oxidation of the GSH pool would dramatically change this scenario. At a physiological concentration of 2 m*M* GSH, oxidation of only 2% GSH would produce 20 μM GSSG and establish a GSH/GSSG of 100. In equilibrium with this GSH/GSSG ratio, glutathionylated GrxS12 would exceed reduced GrxS12, and this effect would be more pronounced at neutral than alkaline pH. As a result, a very limited oxidation of the GSH pool could lead to a strong inhibition of GrxS12 activity *in vivo*. Such inhibition would be stronger in the dark, when a neutral pH is established in chloroplasts, than in the light, when the photosynthetic activity tends to increase the stromal pH by about one unit (47).

A major difference between GrxS12 and other chloroplast Grxs of higher plants may reside in the stability of the glutathionylated form. Only monothiolic Grx such as GrxS12 can exist in a stable glutathionylated form, because, even in the absence of GSH, glutathionylation of dithiol Grxs could be slowly removed by formation of an intramolecular disulfide between the two active Cys. Glutathionylation of GrxS12 can result from either reaction with H_2O_2 and GSH (9), or GSSG, or GSNO or by interaction with a glutathionylated substrate (A_4-glyceraldehyde-3-phosphate dehydrogenase, (9); ICL, BSA, this work). Stability of GrxS12-SSG depends on pH and [GSH]/[GSSG] ratios and is, thus, predicted to increase in the dark and under stress conditions that could lower the [GSH]/[GSSG] ratio. Notably, the only Grx identified to date as a target of glutathionylation under stress by proteomic approaches in higher plants is indeed GrxS12 (13) and we speculate that GrxS12-SSG may be involved in signaling.

In this scenario, the unique biochemical properties of GrxS12 would allow glutathione to play a signaling role through glutathionylation of GrxS12 targets. The rapid inactivation of GrxS12 by glutathionylation under mild oxidative stress would stabilize a number of glutathionylated proteins that could propagate the oxidative stress signal and possibly trigger-specific adaptative responses. Once these responses have been initiated, the decrease of the intracellular redox potential to a more reduced state should lead to reactivation of GrxS12 and deglutathionylation of GrxS12 targets. This proposed mechanism involving GrxS12 inactivation in signaling shares some similarities with the inactivation of 2-Cys peroxiredoxin (Prx) by overoxidation or phosphorylation (40). Indeed, it has been proposed that overoxidation of the peroxidatic Cys of 2-Cys Prx to the sulfinate form and its subsequent slow reduction by sulfiredoxin (5, 50) could lead to transient accumulation of H_2O_2 and thereby allow H_2O_2 to play a signaling role. This concept has been termed the "floodgate" hypothesis (52). However, in the case of receptor signaling, another mechanism appears to be involved, as a membrane-associated 2-Cys Prx was recently shown to be reversibly inactivated by phosphorylation in cells stimulated *via* growth factors or immune receptors (51). This localized inactivation of 2-Cys Prx likely allows generating favorable H_2O_2 gradients around membranes, where signaling proteins are concentrated, while minimizing the general accumulation of H_2O_2 to toxic levels.

Similarly, the unique biochemical properties of GrxS12 may allow this enzyme to facilitate redox signaling by allowing accumulation of glutathionylated proteins, as just mentioned. Other chloroplastic Grxs may either exhibit distinct specificities or be regulated by other mechanisms such as binding to Fe-S clusters that has been suggested to constitute a mechanism of regulation of Grx activity (4). Confirming the potential contribution of GrxS12 in redox signaling will require determining GrxS12-specific targets and analyzing the regulation of Grx activities *in vivo*. Finally, as GrxS12 orthologs are absent in green algae (30), its potential role as a facilitator of redox sensing and signaling in chloroplasts may be linked to the requirement for a tighter redox control in terrestrial plants, as previously suggested by the analysis of some redox-controlled Calvin cycle enzymes (31).

Materials and Methods

Materials and enzymes

NAP-5 columns and 5,5′-dithiobis-2-nitrobenzoic acid (DTNB) were purchased from GE Healthcare (Piscataway, NJ

USA) and Pierce (Rockford, IL), respectively. GSH and GSSG were purchased from either Roche Diagnostics Corporation (Indianapolis, IN) or Sigma-Aldrich (St. Louis, MO). All other chemicals were obtained from Sigma-Aldrich.

GR from baker's yeast and bovine catalase were purchased from Sigma (St. Louis, MO). Recombinant ICL from *C. reinhardtii* (ICL) was purified as described in (3). Poplar GrxS12 wild type (GrxS12) and mutants GrxS12-C29S (C29S) and GrxS12-C87S (C87S) were expressed and purified as previously described (9). Purity of all Grx forms used in this work was assessed by SDS-PAGE and Coomassie blue staining (Supplementary Fig. S1; Supplementary Data are available online at www.liebertonline.com/ars). Concentration of purified proteins was determined from UV absorption at 280 nm, and extinction coefficients were calculated from the sequence ($\varepsilon = 64{,}540$ and 9970 M^{-1} cm^{-1} for ICL and GrxS12, respectively).

Preparation of BSA-SSG

BSA-SSG was prepared by treating the protein with 20 m*M* reduced DTT for 30 min at room temperature followed by desalting on a NAP-5 column pre-equilibrated with 30 m*M* Tris-HCl, pH 7.9. The reduced protein was then allowed to react with a 50-fold molar excess of GSSG for 16 h at room temperature and desalted as just described. The degree of BSA glutathionylation was spectrophotometrically determined by following NADPH oxidation at 340 nm in a cuvette containing 0.2 m*M* NADPH, 0.5 m*M* GSH, 6 μg/ml GR, 25 n*M* GrxS12 wt, and a varying concentration of BSA-SSG. The BSA was quantified at 280 nm ($\varepsilon = 43{,}600$ M^{-1} cm^{-1}), and the concentration of protein-bound GSH groups was calculated from the total NADPH consumption for each BSA concentration as described in (6). This procedure resulted in 1.03 ± 0.08 GSH per molecule of BSA (Supplementary Fig. S2), consistent with monoglutathionylation of the protein, although some heterogeneity in BSA-SSG preparations cannot be excluded.

Activity measurements and determination of apparent kinetic parameters

Before activity measurements, GrxS12 and its variants were incubated with 10 m*M* DTT for 30 min at room temperature and desalted on a NAP-5 column pre-equilibrated in 30 m*M* Tris-HCl, pH 7.9. Grx activity in the HED assay was determined as previously described (54). Briefly, 0.7 m*M* HED was added to a mixture containing 100 m*M* Tris-HCl, pH 7.9, 2 m*M* EDTA, 0.1 mg/ml BSA, 0.2 m*M* NADPH, 1 m*M* GSH, and 6 μg/ml GR. After 3 min of preincubation, 30 n*M* GrxS12 was added to the sample cuvette, and buffer was added to the reference cuvette. This GrxS12 concentration was previously checked for being within the range of linear responses of activity *versus* enzyme concentration. The decrease in absorbance was followed at 340 nm. GRX activity was determined after subtracting the spontaneous reduction rate observed in the absence of Grx, and the number of μmoles of NADPH oxidized per second per μmole of enzyme (*i.e.,* turnover number, s^{-1}) was calculated using the extinction coefficient of NADPH ($\varepsilon_{340} = 6230$ M^{-1} cm^{-1}). The apparent K_m for glutathione of C87S mutant was determined as previously described (9). Apparent kinetic parameters for glutathionylated substrates were determined using either HED (0.1– 1.5 m*M*) or BSA-SSG (2.5–50 μM) in a mixture of 100 m*M* Tris-HCl, pH 7.9, 2 m*M* EDTA, 0.1 mg/ml BSA, 0.2 m*M* NADPH, 6 μg/ml GR plus 1 m*M* GSH, and 30 n*M* GrxS12. Three independent experiments were performed at each substrate concentration, and the apparent K_m and k_{cat} values were calculated by nonlinear regression using a Michaelis Menten equation with the program CoStat (CoHort software, Monterey, CA).

Two-substrate kinetic analysis

The catalytic mechanism of GrxS12 was determined by independently varying the concentration of BSA-SSG and GSH to produce a 4×4 matrix of concentration sets. Deglutathionylation activity was determined as just described with 30 n*M* GrxS12. Each individual data set for a varied substrate at a fixed concentration of the other substrate was analyzed by nonlinear regression analysis as just described. A pair of apparent k_{cat} and apparent K_m values was, thus, obtained at each single concentration of the fixed substrate. Apparent k_{cat} values obtained in different experiments under identical conditions were averaged ($\pm$SD) and represented in secondary plots ($1/k_{cat}$ *vs.* 1/[substrate]), from which the kinetic efficiency parameters k_{cat}/K_m were derived.

Reactivation of ICL-SSG by GrxS12 and its variants

ICL-SSG was prepared as described in (3). All reactivation treatments were performed in 50 m*M* HEPES-NaOH, pH 7.2 at room temperature. Reactivation of ICL-SSG (10 μM) was measured with GrxS12 (5 or 0.1 μM) or C87S (5 μM) or C29S (5 μM) in the presence of 0.5 m*M* DTT or 2 m*M* GSH alone or 2 m*M* GSH in the presence of a GRS made of 0.2 m*M* NADPH and 6 μg/ml GR. Control reaction mixtures were performed in the same conditions by omitting Grxs. At indicated times, aliquots were withdrawn to assay ICL activity monitored as described in (3). Half-saturating concentration for GrxS12 and C87S mutant were determined by incubating ICL-SSG (10 μM) in the presence of varying concentrations of GrxS12 and C87S mutant (0.5 to 20 μM) and 2 m*M* GSH alone, or with GRS.

Influence of the [GSH]/[GSSG] ratio on GrxS12-dependent deglutathionylation of ICL-SSG

ICL-SSG (10 μM) was incubated in the presence of 5 μM GrxS12 and different [GSH]/[GSSG] ratios at a total concentration of 2 m*M*. After 15 min incubation, aliquots were withdrawn to assay ICL activity monitored as described in Ref. (3). Control experiments were carried out by incubating reduced ICL (10 μM) with different [GSH]/[GSSG] ratios (as just described), and protein activity was measured after 15 min incubation. Freshly prepared solutions of GSH invariably contain small amounts of GSSG, which was determined by either directly assaying GSH with DTNB (54) or by enzymatic assay of GSSG by GR (1 μg/ml) and NADPH (0.2 m*M*). The degree of GSSG contamination was found between 0.5% and 1% on a molar basis, and this value was considered to calculate the effective [GSH]/[GSSG] ratio for each reaction mixture.

pH-dependence of GrxS12 activity

To measure the pH-dependency of GrxS12-catalyzed deglutathionylation, HED assays were performed as just

described except that β-ME-SSG was generated in a mixture containing 100 m*M* Tris-HCl, pH 7.9, 2 m*M* EDTA, 7 m*M* HED, and 10 mM GSH. After preincubation (3 min), Grx activity was determined by adding 50 μl of the preincubation mixture to 450 μl of the spectrophotometer assay system containing 0.1 mg/ml BSA, 0.2 m*M* NADPH, and GR (6 or 90 μg/ml). The following buffers were used: potassium phosphate at pH 6.5–7.5; Tris-HCl at pH 7.5–9; and glycine at pH 9–10. Rates of GrxS12-dependent deglutathionylation were represented as a percentage of maximal activity. Plots of activity *versus* pH were fit to a derivation of the Henderson-Hasselbalch equation as in (18).

Determination of the pK_a of the catalytic Cys of GrxS12 by IAM inactivation

The pH-dependence of inactivation of GrxS12 and C87S mutant by IAM was carried out by incubating reduced proteins (3 μ*M*) with or without IAM (0.3 m*M*) for 3 min in sodium citrate or phosphate buffer ranging from pH 2 to 6.5 (18). After preincubation, Grx activity was determined by adding an aliquot of the preincubation mixture to the HED assay system just described. The residual activity expressed as a percentage of maximal activity was plotted *versus* pH, and an adaptation of the Henderson-Hasselbalch equation was used to calculate the pK_a of the active site Cys as in (18).

IAM-dependent inactivation kinetics

Reduced GrxS12 (3 μ*M*) was incubated in 30 m*M* Tris-HCl, pH 7.9, in the presence of IAM ranging from 25 to 250 μ*M* at room temperature. All reactions were initiated by the addition of IAM. At different times, aliquots were withdrawn from the incubation mixture and diluted 100-fold into the standard HED assay system, and enzyme activity was determined. All inactivation experiments were performed in triplicate and monitored relative to a control sample without IAM, which is set to 100% activity at each time point. Estimates of the concentration of IAM that gives half-maximal rate of inactivation (K_I) and first-order inactivation rate constants (k_{inact}) were determined according to the Kitz-Wilson plot (29).

Effect of hydrogen peroxide and GSNO on GrxS12

Reduced GrxS12 (3 μ*M*) was treated with H_2O_2 ranging from 25 μ*M* to 1 m*M* or with 0.1 m*M* H_2O_2 in the presence of 0.5 m*M* GSH in 30 m*M* Tris-HCl (pH 7.9) at room temperature. At different times, enzyme activity was determined as just described, and H_2O_2-dependent inactivation kinetics were analyzed as described in the previous section (29). In a separate set of control experiments, it was demonstrated that GR activity is not sensitive to the highest concentration of H_2O_2 used (1 m*M*) after 100-fold dilution in an assay cuvette system containing 0.2 m*M* NADPH and 50 μ*M* GSSG in 100 m*M* Tris-HCl, pH 7.9 (data not shown). For reduction of oxidized proteins, H_2O_2-treated samples were incubated for 15 min at room temperature with the GRS (1 m*M* GSH, 0.2 m*M* NADPH, and 6 μg/ml GR) in the presence of 100 U/ml bovine catalase.

To study S-nitrosylation, reduced GrxS12 was incubated with 0.5 m*M* GSNO in PBS (137 m*M* NaCl, 2.7 m*M* KCl, 8.1 m*M* Na_2HPO_4, and 1.9 m*M* KH_2PO_4), pH 7.4, 1 m*M* EDTA at room temperature and enzyme activity was assayed at different incubation times. S-nitrosylation of GrxS12 was analyzed by recording the UV-visible spectra of the protein treated with 0.5 m*M* GSNO for 1 h and desalted on a NAP-5 column equilibrated with PBS buffer. The desalted protein sample was also used for MALDI-TOF mass spectrometry analysis as described in (41).

Determination of K_{ox} and midpoint redox potential of GrxS12 by MALDI-TOF mass spectrometry in the presence of GSH

The redox potential of the mixed disulfide of GrxS12-SSG was calculated after equilibration with different [GSH]/[GSSG] ratios. A MALDI-TOF mass spectrometry approach was developed to quantify in each sample the ratio of reduced (GrxS12-SH) and glutathionylated GrxS12 (GrxS12-SSG) from the area of the corresponding peaks, which were separated by approx 305 Da in mass. As observed by Iversen *et al.* (25), even in completely glutathionylated samples, small amounts of reduced protein were always detected, suggesting that approximately 5% of mixed disulfide bonds were broken by lazer shooting (37). The relative amounts of GrxS12-SH and GrxS12-SSG were, thus, determined by numeric integration of the peak areas after correction for the fraction of GrxS12-SH, which was calculated to derive from GrxS12-SSG disulfide breakage by shooting. The equilibrium constant of the reaction of GrxS12 with GSSG is defined as follows:

$$K_{ox} = [\text{GrxS12-SSG}]/[\text{GrxS12-SH}] \times [\text{GSH}]/[\text{GSSG}]$$

For determination of the K_{ox}, reduced GrxS12 (50 μ*M*) was incubated in 30 m*M* Tris-HCl (pH 7.9) with different [GSH]/[GSSG] ratios, and the relative amounts of GrxS12-SH and GrxS12-SSG were measured as just described. GrxS12 was added to each mix of glutathione and allowed to equilibrate for 10 min before the reaction was quenched by 1.3% trifluoroacetic acid. Samples from each acid-quenched reaction were analyzed as described in (45). The equilibrium concentrations of GSH were calculated by considering the amount of GSH released by the reaction of GSSG with GrxS12-SH. Conversely, the equilibrium concentration of GSSG was calculated after subtracting from the initial concentration of GSSG, an amount of GSSG equal to the amount of GrxS12-SSG at equilibrium.

The standard redox potential of GrxS12 mixed disulfide was derived from the K_{ox} according to the Nernst equation. The standard redox potential of the GSH/GSSG couple at pH 7.9 was considered to be −295 mV, that is, 55 mV more negative than at pH 7.0 (−240 mV) (1) based on the assumption that GSH is fully protonated at pH 7.9 ($pK_{a(GSH)} \approx 8.7$) (46); and, therefore, the pH-dependence of $E_{m(GSH/GSSG)}$ between 7.0 and 7.9 should be linear with a slope of −60 mV per pH unit.

Determination of the standard redox potential of GrxS12 by tryptophan intrinsic fluorescence and pH-dependence of the K_{ox}

Fluorescence measurements were performed at 25°C in quartz cuvettes with 1 cm light-path length. The excitation wavelength was set at 295 nm (for selective observation of the tryptophan residue), and the emission was recorded between 300 and 450 nm with a bandwidth of 10 nm at a scan speed of 50 nm/min. To calibrate the measurements, the fluorescence

signals of fully reduced and fully glutathionylated GrxS12 (0.4 μM) were recorded under native conditions in 30 mM Tris-HCl, pH 7.9, 1 mM EDTA. Buffer blanks were run for each sample and were subtracted from the spectra.

The pH dependence of the K_{ox} of GrxS12 with GSH/GSSG as redox buffer was determined at different pH values by the tryptophan intrinsic fluorescence method. Concentration of all buffers was 100 mM: sodium citrate, pH 5.0; MES, pH 6.0; HEPES, pH 7.0; Tris-HCl, pH 7.9; glycine, pH 9.0. The reduced protein (20 μM) was allowed to equilibrate for 1 h in the presence of an initial [GSH]/[GSSG] ratio of 200:1. Afterward, fluorescence spectra were recorded in 10-fold diluted samples in the same buffer as the incubation. For each sample, the fluorescence signal was measured at 345 nm (excitation at 295 nm), which corresponds to GrxS12 maximum fluorescence peak.

Acknowledgments

This work was supported in part by PRIN 2008 grant (to M.Z. and P.T.) from the Ministero dell'Istruzione, dell'Università e della Ricerca of Italy, by ANR Grant 08-BLAN-0153 GLUTAPHOTO (to M.B. and S.D.L.) and by ANR JC07 204825 (to J.C. and N.R.).

Author Disclosure Statement

The authors have no conflict of interest to disclose.

References

1. Åslund F, Berndt KD, and Holmgren A. Redox potentials of glutaredoxins and other thiol-disulfide oxidoreductases of the thioredoxin superfamily determined by direct protein-protein redox equilibria. *J Biol Chem* 272: 30780–30786, 1997.
2. Bandyopadhyay S, Gama F, Molina-Navarro MM, Gualberto JM, Claxton R, Naik SG, Huynh BH, Herrero E, Jacquot JP, Johnson MK, and Rouhier N. Chloroplast monothiol glutaredoxins as scaffold proteins for the assembly and delivery of [2Fe-2S] clusters. *EMBO J* 27: 1122–1133, 2008.
3. Bedhomme M, Zaffagnini M, Marchand CH, Gao XH, Moslonka-Lefebvre M, Michelet L, Decottignies P, and Lemaire SD. Regulation by glutathionylation of isocitrate lyase from *Chlamydomonas reinhardtii*. *J Biol Chem* 284: 36282–36291, 2009.
4. Berndt C, Hudemann C, Hanschmann EM, Axelsson R, Holmgren A, and Lillig CH. How does iron-sulfur cluster coordination regulate the activity of human glutaredoxin 2? *Antioxid Redox Signal* 9: 151–157, 2007.
5. Biteau B, Labarre J, and Toledano MB. ATP-dependent reduction of cysteine-sulphinic acid by *S. cerevisiae* sulphiredoxin. *Nature* 425: 980–984, 2003.
6. Ceylan S, Seidel V, Ziebart N, Berndt C, Dirdjaja N, and Krauth-Siegel RL. The dithiol glutaredoxins of African trypanosomes have distinct roles and are closely linked to the unique trypanothione metabolism. *J Biol Chem* 285: 35224–35237, 2010.
7. Colman R. Glutathione reductase (Yeast). *Methods Enzymol* 17: 500–503, 1971.
8. Couturier J, Jacquot JP, and Rouhier N. Evolution and diversity of glutaredoxins in photosynthetic organisms. *Cell Mol Life Sci* 66: 2539–2557, 2009.
9. Couturier J, Koh CS, Zaffagnini M, Winger AM, Gualberto JM, Corbier C, Decottignies P, Jacquot JP, Lemaire SD, Didierjean C, and Rouhier N. Structure-function relationship of the chloroplastic glutaredoxin S12 with an atypical WCSYS active site. *J Biol Chem* 284: 9299–9310, 2009.
10. Cowgill RW. Fluorescence and the structure of proteins. XII. Pancreatic trypsin inhibitor. *Biochim Biophys Acta* 140: 552–554, 1967.
11. Dalle-Donne I, Rossi R, Colombo G, Giustarini D, and Milzani A. Protein S-glutathionylation: a regulatory device from bacteria to humans. *Trends Biochem Sci* 34: 85–96, 2009.
12. Discola KF, de Oliveira MA, Rosa Cussiol JR, Monteiro G, Barcena JA, Porras P, Padilla CA, Guimaraes BG, and Netto LE. Structural aspects of the distinct biochemical properties of glutaredoxin 1 and glutaredoxin 2 from Saccharomyces cerevisiae. *J Mol Biol* 385: 889–901, 2009.
13. Dixon DP, Skipsey M, Grundy NM, and Edwards R. Stress-induced protein S-glutathionylation in Arabidopsis. *Plant Physiol* 138: 2233–2244, 2005.
14. Fernandes AP and Holmgren A. Glutaredoxins: glutathione-dependent redox enzymes with functions far beyond a simple thioredoxin backup system. *Antioxid Redox Signal* 6: 63–74, 2004.
15. Foyer CH and Noctor G. Redox homeostasis and antioxidant signaling: a metabolic interface between stress perception and physiological responses. *Plant Cell* 17: 1866–1875, 2005.
16. Foyer CH and Noctor G. Redox regulation in photosynthetic organisms: signaling, acclimation, and practical implications. *Antioxid Redox Signal* 11: 861–905, 2009.
17. Foyer CH and Noctor G. Ascorbate and glutathione: the heart of the redox hub. *Plant Physiol* 155: 2–18, 2011.
18. Gallogly MM, Starke DW, Leonberg AK, Ospina SM, and Mieyal JJ. Kinetic and mechanistic characterization and versatile catalytic properties of mammalian glutaredoxin 2: implications for intracellular roles. *Biochemistry* 47: 11144–11157, 2008.
19. Gallogly MM, Starke DW, and Mieyal JJ. Mechanistic and kinetic details of catalysis of thiol-disulfide exchange by glutaredoxins and potential mechanisms of regulation. *Antioxid Redox Signal* 11: 1059–1081, 2009.
20. Gao X, Bedhomme, M, Michelet, L, Zaffagnini, M, and Lemaire, SD. Glutathionylation in photosynthetic organisms. *Adv Bot Res* 52: 363–403, 2009.
21. Gao XH, Zaffagnini M, Bedhomme M, Michelet L, Cassier-Chauvat C, Decottignies P, and Lemaire SD. Biochemical characterization of glutaredoxins from *Chlamydomonas reinhardtii*: kinetics and specificity in deglutathionylation reactions. *FEBS Lett* 584: 2242–2248, 2010.
22. Ghezzi P. Regulation of protein function by glutathionylation. *Free Radic Res* 39: 573–580, 2005.
23. Gravina SA and Mieyal JJ. Thioltransferase is a specific glutathionyl mixed disulfide oxidoreductase. *Biochemistry* 32: 3368–3376, 1993.
24. Hirasawa M, Schürmann P, Jacquot JP, Manieri W, Jacquot P, Keryer E, Hartman FC, and Knaff DB. Oxidation-reduction properties of chloroplast thioredoxins, ferredoxin:thioredoxin reductase, and thioredoxin f-regulated enzymes. *Biochemistry* 38: 5200–5205, 1999.
25. Iversen R, Andersen PA, Jensen KS, Winther JR, and Sigurskjold BW. Thiol-disulfide exchange between glutaredoxin and glutathione. *Biochemistry* 49: 810–820, 2010.
26. Jensen KS, Hansen RE, and Winther JR. Kinetic and thermodynamic aspects of cellular thiol-disulfide redox regulation. *Antioxid Redox Signal* 11: 1047–1058, 2009.
27. Johansson C, Lillig CH, and Holmgren A. Human mitochondrial glutaredoxin reduces S-glutathionylated proteins with high affinity accepting electrons from either glutathione or thioredoxin reductase. *J Biol Chem* 279: 7537–7543, 2004.

28. Jubany-Mari T, Alegre-Batlle L, Jiang K, and Feldman LJ. Use of a redox-sensing GFP (c-roGFP1) for real-time monitoring of cytosol redox status in *Arabidopsis thaliana* water-stressed plants. *FEBS Lett* 584: 889–897, 2010.
29. Kitz R and Wilson IB. Esters of methanesulfonic acid as irreversible inhibitors of acetylcholinesterase. *J Biol Chem* 237: 3245–3249, 1962.
30. Lemaire SD. The glutaredoxin family in oxygenic photosynthetic organisms. *Photosynth Res* 79: 305–318, 2004.
31. Marri L, Zaffagnini M, Collin V, Issakidis-Bourguet E, Lemaire SD, Pupillo P, Sparla F, Miginiac-Maslow M, and Trost P. Prompt and easy activation by specific thioredoxins of calvin cycle enzymes of *Arabidopsis thaliana* associated in the GAPDH/CP12/PRK supramolecular complex. *Mol Plant* 2: 259–269, 2009.
32. Meyer AJ, Brach T, Marty L, Kreye S, Rouhier N, Jacquot JP, and Hell R. Redox-sensitive GFP in *Arabidopsis thaliana* is a quantitative biosensor for the redox potential of the cellular glutathione redox buffer. *Plant J* 52: 973–986, 2007.
33. Mhamdi A, Hager J, Chaouch S, Queval G, Han Y, Taconnat L, Saindrenan P, Gouia H, Issakidis-Bourguet E, Renou JP, and Noctor G. Arabidopsis GLUTATHIONE REDUCTASE1 plays a crucial role in leaf responses to intracellular hydrogen peroxide and in ensuring appropriate gene expression through both salicylic acid and jasmonic acid signaling pathways. *Plant Physiol* 153: 1144–1160, 2010.
34. Michelet L, Zaffagnini M, Marchand C, Collin V, Decottignies P, Tsan P, Lancelin JM, Trost P, Miginiac-Maslow M, Noctor G, and Lemaire SD. Glutathionylation of chloroplast thioredoxin f is a redox signaling mechanism in plants. *Proc Natl Acad Sci U S A* 102: 16478–16483, 2005.
35. Michelet L, Zaffagnini M, Vanacker H, Le Marechal P, Marchand C, Schroda M, Lemaire SD, and Decottignies P. *In vivo* targets of S-thiolation in *Chlamydomonas reinhardtii*. *J Biol Chem* 283: 21571–2158, 2008.
36. Mieyal JJ, Starke DW, Gravina SA, Dothey C, and Chung JS. Thioltransferase in human red blood cells: purification and properties. *Biochemistry* 30: 6088–6097, 1991.
37. Patterson SD and Katta V. Prompt fragmentation of disulfide-linked peptides during matrix-assisted laser desorption ionization mass spectrometry. *Anal Chem* 66: 3727–3732, 1994.
38. Poole LB and Nelson KJ. Discovering mechanisms of signaling-mediated cysteine oxidation. *Curr Opin Chem Biol* 12: 18–24, 2008.
39. Queval G, Jaillard D, Zechmann B, and Noctor G. Increased intracellular HO availability preferentially drives glutathione accumulation in vacuoles and chloroplasts. *Plant Cell Environ* 34: 21–32, 2011.
40. Rhee SG and Woo HA. Multiple functions of peroxiredoxins: peroxidases, sensors and regulators of the intracellular messenger H_2O_2, and protein chaperones. *Antioxid Redox Signal* 15: 781–794, 2011.
41. Rouhier N. Plant glutaredoxins: pivotal players in redox biology and iron-sulphur centre assembly. *New Phytol* 186: 365–372, 2010.
42. Rouhier N, Couturier J, and Jacquot JP. Genome-wide analysis of plant glutaredoxin systems. *J Exp Bot* 57: 1685–1696, 2006.
43. Rouhier N, Gelhaye E, and Jacquot JP. Plant glutaredoxins: still mysterious reducing systems. *Cell Mol Life Sci* 61: 1266–1277, 2004.
44. Rouhier N, Lemaire SD, and Jacquot JP. The role of glutathione in photosynthetic organisms: emerging functions for glutaredoxins and glutathionylation. *Annu Rev Plant Biol* 59: 143–166, 2008.
45. Sicard-Roselli C, Lemaire S, Jacquot JP, Favaudon V, Marchand C, and Houee-Levin C. Thioredoxin Ch1 of *Chlamydomonas reinhardtii* displays an unusual resistance toward one-electron oxidation. *Eur J Biochem* 271: 3481–3487, 2004.
46. Srinivasan U, Mieyal PA, and Mieyal JJ. pH profiles indicative of rate-limiting nucleophilic displacement in thiol-transferase catalysis. *Biochemistry* 36: 3199–3206, 1997.
47. Takizawa K, Cruz JA, Kanazawa A, and Kramer DM. The thylakoid proton motive force *in vivo*. Quantitative, non-invasive probes, energetics, and regulatory consequences of light-induced pmf. *Biochim Biophys Acta* 1767: 1233–1244, 2007.
48. Tamarit J, Belli G, Cabiscol E, Herrero E, and Ros J. Biochemical characterization of yeast mitochondrial Grx5 monothiol glutaredoxin. *J Biol Chem* 278: 25745–25751, 2003.
49. Tarrago L, Laugier E, Zaffagnini M, Marchand C, Le Marechal P, Rouhier N, Lemaire SD, and Rey P. Regeneration mechanisms of *Arabidopsis thaliana* methionine sulfoxide reductases B by glutaredoxins and thioredoxins. *J Biol Chem* 284: 18963–18971, 2009.
50. Woo HA, Chae HZ, Hwang SC, Yang KS, Kang SW, Kim K, and Rhee SG. Reversing the inactivation of peroxiredoxins caused by cysteine sulfinic acid formation. *Science* 300: 653–656, 2003.
51. Woo HA, Yim SH, Shin DH, Kang D, Yu DY, and Rhee SG. Inactivation of peroxiredoxin I by phosphorylation allows localized H(2)O(2) accumulation for cell signaling. *Cell* 140: 517–528, 2010.
52. Wood ZA, Poole LB, and Karplus PA. Peroxiredoxin evolution and the regulation of hydrogen peroxide signaling. *Science* 300: 650–653, 2003.
53. Zaffagnini M, Michelet L, Marchand C, Sparla F, Decottignies P, Le Marechal P, Miginiac-Maslow M, Noctor G, Trost P, and Lemaire SD. The thioredoxin-independent isoform of chloroplastic glyceraldehyde-3-phosphate dehydrogenase is selectively regulated by glutathionylation. *FEBS J* 274: 212–226, 2007.
54. Zaffagnini M, Michelet L, Massot V, Trost P, and Lemaire SD. Biochemical characterization of glutaredoxins from *Chlamydomonas reinhardtii* reveals the unique properties of a chloroplastic CGFS-type glutaredoxin. *J Biol Chem* 283: 8868–8876, 2008.

Address correspondence to:
Prof. Paolo Trost
Department of Experimental Evolutionary Biology
University of Bologna
Via Irnerio 42
I-40126 Bologna
Italy

E-mail: paolo.trost@unibo.it

Dr. Stéphane D. Lemaire
Laboratoire de Biologie Moléculaire et Cellulaire des Eucaryotes
FRE3354 CNRS/UPMC
Institut de Biologie Physico-Chimique
13 rue Pierre et Marie Curies
75005 Paris
France

E-mail: stephane.lemaire@ibpc.fr

Date of first submission to ARS Central, February 2, 2011; date of final revised submission, June 24, 2011; date of acceptance, June 27, 2011.

Abbreviations Used

β-ME-SSG = glutathionylated β-mercaptoethanol.
BSA = bovine serum albumin
BSA-SSG = glutathionylated bovine serum albumin
Cys = cysteine
DTNB = 5,5′-dithiobis-2-nitrobenzoic acid
DTT = dithiothreitol
FTR = ferredoxin:thioredoxin reductase
GR = glutathione reductase
GRS = GSH-regenerating system
Grx = glutaredoxin
GSH = glutathione (reduced form)
GSNO = nitrosoglutathione
GSSG = glutathione (oxidized form)
HED = hydroxyethyl disulfide
IAM = iodoacetamide
ICL = isocitrate lyase
ICL-SSG = glutathionylated isocitrate lyase
MALDI-TOF = matrix-assisted laser desorption/ionization-time of flight
PDT-bimane = (2-pyridyl)di-thiobimane
Prx = peroxiredoxin
SD = standard deviation

This article has been cited by:

1. Yves Meyer , Christophe Belin , Valérie Delorme-Hinoux , Jean-Philippe Reichheld , Christophe Riondet . 2012. Thioredoxin and Glutaredoxin Systems in Plants: Molecular Mechanisms, Crosstalks, and Functional Significance. *Antioxidants & Redox Signaling* **17**:8, 1124-1160. [Abstract] [Full Text HTML] [Full Text PDF] [Full Text PDF with Links]
2. Marcel Deponte. 2012. Glutathione catalysis and the reaction mechanisms of glutathione-dependent enzymes. *Biochimica et Biophysica Acta (BBA) - General Subjects* . [CrossRef]
3. Elke Ströher, A. Harvey Millar. 2012. The biological roles of glutaredoxins. *Biochemical Journal* **446**:3, 333-348. [CrossRef]
4. Jérémy Couturier, Florence Vignols, Jean-Pierre Jacquot, Nicolas Rouhier. 2012. Glutathione- and glutaredoxin-dependent reduction of methionine sulfoxide reductase A. *FEBS Letters* . [CrossRef]
5. Jay R. Laver , Samantha McLean , Lesley A.H. Bowman , Laura J. Harrison , Robert C. Read , Robert K. Poole . Nitrosothiols in Bacterial Pathogens and Pathogenesis. *Antioxidants & Redox Signaling*, ahead of print. [Abstract] [Full Text HTML] [Full Text PDF] [Full Text PDF with Links]
6. Mariette Bedhomme, Mattia Adamo, Christophe H. Marchand, Jérémy Couturier, Nicolas Rouhier, Stéphane D. Lemaire, Mirko Zaffagnini, Paolo Trost. 2012. Glutathionylation of cytosolic glyceraldehyde-3-phosphate dehydrogenase from the model plant Arabidopsis thaliana is reversed by both glutaredoxins and thioredoxins in vitro. *Biochemical Journal* **445**:3, 337-347. [CrossRef]
7. X.-W. Chi, C.-T. Lin, Y.-C. Jiang, L. Wen, C.-T. Lin. 2012. A dithiol glutaredoxin cDNA from sweet potato (Ipomoea batatas [L.] Lam): enzyme properties and kinetic studies. *Plant Biology* **14**:4, 659-665. [CrossRef]
8. Erin M.G. Allen , John J. Mieyal . Protein-Thiol Oxidation and Cell Death: Regulatory Role of Glutaredoxins. *Antioxidants & Redox Signaling*, ahead of print. [Abstract] [Full Text HTML] [Full Text PDF] [Full Text PDF with Links]
9. John J. Mieyal , P. Boon Chock . 2012. Posttranslational Modification of Cysteine in Redox Signaling and Oxidative Stress: Focus on S-Glutathionylation. *Antioxidants & Redox Signaling* **16**:6, 471-475. [Abstract] [Full Text HTML] [Full Text PDF] [Full Text PDF with Links]
10. Mirko Zaffagnini , Mariette Bedhomme , Christophe H. Marchand , Samuel Morisse , Paolo Trost , Stéphane D. Lemaire . 2012. Redox Regulation in Photosynthetic Organisms: Focus on Glutathionylation. *Antioxidants & Redox Signaling* **16**:6, 567-586. [Abstract] [Full Text HTML] [Full Text PDF] [Full Text PDF with Links]
11. Mirko Zaffagnini, Mariette Bedhomme, Stéphane D. Lemaire, Paolo Trost. 2012. The emerging roles of protein glutathionylation in chloroplasts. *Plant Science* . [CrossRef]